JULY 2018

M.Sc. in BIOCHEMICAL SCIENCE AND TECHNOLOGY

AHMED ISMAIL AL-NUAIMI

UNIVERSITY OF GAZIANTEP

GRADUATE SCHOOL OF NATURAL & APPLIED SCIENCES

REMOVAL OF REACTIVE RED 120 BY USING *MORINGA OLEIFERA* SEEDS

M. Sc. THESIS

IN

BIOCHEMICAL SCIENCE AND TECHNOLOGY

BY

AHMED ISMAIL AL-NUAIMI

JULY 2018

Removal of Reactive Red 120 by Using *Moringa oleifera* Seeds

M.Sc. Thesis

In

Biochemical Science and Technology

University of Gaziantep

Supervisor

Prof. Dr. Abuzer ÇELEKLİ

by

Ahmed Ismail AL-NUAIMI

July 2018

REPUBLIC OF TURKEY
UNIVERSITY OF GAZIANTEP
GRADUATE SCHOOL OF NATURAL & APPLIED SCIENCES
BIOCHEMICAL SCIENCE AND TECHNOLOGY DEPARTMENT

Name of the thesis: Removal of Reactive Red 120 by Using *Moringa oleifera* Seeds

Name of the student: Ahmed Ismail AL-NUAIMI

Exam date: 26/07/2018

Approval of the Graduate School of Natural and Applied Sciences

Prof. Dr. Ahmet Necmeddin YAZICI
Director

I certify that this thesis satisfies all the requirements as a thesis for the degree of Master of Science.

Prof. Dr. Canan CAN
Head of Department

This is to certify that we have read this thesis and that in our consensus opinion it is fully adequate, in scope and quality, as a thesis for the degree of Master of Science.

Prof. Dr. Abuzer ÇELEKLİ
Supervisor

Examining Committee Members:	Signature
Prof. Dr. Canan CAN	.....
Prof. Dr. Abuzer ÇELEKLİ	.....
Assoc. Prof. Dr. Zafer ÇETİN	.....

I hereby declare that all information in this document has been obtained and presented in accordance with academic rules and ethical conduct. I also declare that, as required by these rules and conduct, I have fully cited and referenced all material and results that are not original to this work.

Ahmed Ismail AL-NUAIMI

ABSTRACT

REMOVAL OF REACTIVE RED 120 BY USING *MORINGA OLEIFERA* SEEDS

AL-NUAIMI, Ahmed Ismail
M.Sc. in Biochemical Science and Technology
Supervisor: Prof. Dr. Abuzer ÇELEKLİ
July 2018
57 page

Miracle tree (*Moringa oleifera*) seed has been found useful both economically and medicinally. *M. oleifera* (MO) is a natural plant which is indigenous to south Asia. Its have active bio-coagulate compounds that can be used for water purification since it reduces the use of chemical coagulants. In this study, sorption of Reactive Red (RR) 120 on MO seed was investigated as a function of particle size, adsorbent dose, initial pH level, temperature, initial dye concentration, and contact time. Characterization of the adsorbent was confirmed by FTIR-ATR and SEM spectrum. Results of FTIR-ATR indicated that amino, carbonyl and amide groups play significant role on the sorption of RR 120. Zero-point charge (pH_{zpc}) of MO seed was found as pH 4.5. Increasing initial dye concentration caused to increase dye uptake ($p<0.01$) on the adsorbent. Maximum adsorption of RR 120 on MO seed was found to be at pH 1.0. Logistic and pseudo second order kinetic models showed to well fit for experimental kinetic data. The process was very fast initially, reached equilibrium within 30 min and was well represented by the Logistic equation. Experimental data were analyzed by Langmuir and Freundlich isotherms. According to values of error function and determination of coefficient, Freundlich model was more appropriate isotherm to describe the adsorption of RR 120 on MO seed. The maximum adsorption capacity of RR 120 on MO seed was determined as 412.32 mg g^{-1}. Results indicated that this adsorbent had a great potential for removing of RR 120 as an eco-friendly process.

Key Words: *Moringa oleifera*, Reactive Red 120, Dyes, Wastewater, Purification.

ÖZET

MORINGA OLEIFERA TOHUMLARI KULLANARAK REAKTİF KIRMIZI 120 UZAKLAŞTIRILMASI

AL-NUAIMI, Ahmed Ismail

Yüksek Lisans Tezi, Biyokimyasal Bilim ve Teknoloji

Tez Yöneticisi: Prof. Dr. Abuzer ÇELEKLİ

Temmuz 2018

57 sayfa

Mucize ağacı (*Moringa oleifera)* tohumunun hem ekonomik hem de tıbbi olarak yararlı olduğu bulunmuştur. *M. oleifera*, Güney Asya'ya özgü doğal bir bitkidir. Kimyasal pıhtılaşma maddelerinin kullanımını azalttığı için su arıtmada kullanılabilen aktif biyo-pıhtılaştırıcı bileşiklere sahiptir. Bu çalışmada, *M. oleifera* (MO) tohumunda Reaktif Kırmızı (RR) 120'nin partikül büyüklüğü, adsorban dozu, başlangıç pH seviyesi, sıcaklık, başlangıçtaki boya konsantrasyonu ve temas süresi gibi bir fonksiyonu araştırılmıştır. Adsorbentin karakterizasyonu FTIR-ATR ve SEM spektrumu ile doğrulandı. FTIR-ATR'nin sonuçları, RR 120'nin emilmesi üzerinde amino, karbonil ve amid gruplarının önemli rol oynadığını gösterdi. MO tohumu'nun sıfir noktası yükü (pHzpc), pH 4.5 olarak bulundu. Başlangıçtaki boya konsantrasyonunun arttırılması, adsorban üzerinde boya alımının artmasına ($p < 0.01$) neden olmuştur. MO tohumu üzerindeki RR 120'nin maksimum adsorpsiyonu, pH 1.0'da bulunmuştur. Lojistik ve sözde ikinci derece kinetik modeller, deneysel kinetik verilere iyi uyum gösterdi. İşlem başlangıçta çok hızlıydı, 30 dakika içinde dengeye ulaştı ve Lojistik denklem tarafından iyi temsil edildi. Deneysel veriler Langmuir ve Freundlich izotermleri ile analiz edildi. Hata fonksiyonuna ve katsayıların belirlenmesine göre, Freundlich modeli, RR 120'nin MO tohumu üzerindeki adsorpsiyonunu tanımlamak için daha uygun izotermdir. MO tohumu üzerindeki RR 120'nin maksimum adsorpsiyon kapasitesi 412.32 mg g-1 olarak belirlenmiştir. Sonuçlar, bu adsorbanın RR 120'nin çevre dostu bir işlem olarak çıkarılması için büyük bir potansiyele sahip olduğunu gösterdi.

Anahtar Kelimeler: *Moringa oleifera*, Reaktif kırmızı 120, Boyalar, Atıksu, Arıtma.

ACKNOWLEDGEMENTS

I acknowledge with deeply gratitude and appreciation to my supervisor Prof. Dr. Abuzer ÇELEKLİ, his guidance, excellent advise and cooperation during the course of this work. He has followed my work step by step so that I'm extremely grateful and indebted to him for his expert extended to me. His timely and efficient contribution helped me shape this thesis into its final form.

I would like to express my deep appreciation to my family and my friends for their support to me during my whole time study.

TABLE OF CONTENTS

LIST OF TABLES

LIST OF FIGURES

CHAPTER I
INTRODUCTION

1.1 Water Pollution

With scientific progress, industrial developments have left their negative impact on the environment. Direct disposal of waste from various factories causes pollution of water systems due to the use of different types of hazardous dyes on human life. Wastewater contains organic compounds with toxic color (Mohan et al., 2007). There is a negative impact on people who use liquid wastewater for washing, drinking, and bathing because has contained toxic dyes (Sharma et al., 2000). This water is dangerous and not suitable for human use, even if it contains a 1.0 mg/L of industrial dye, so check the water quality before use (Malik et al., 2007). In addition, the presence of industrial dyes in aquatic ecosystems, affects directly the transmission of sunlight to water and indirectly the plants photosynthesis process. These toxic dyes have effects on aquatic life; by toxicity for all aquatic biota.

Due to their; toxic compounds transfers to the human via food net, toxic dyes could cause kidney and liver cancer, and effects the reproductive and the central nervous system (Kadirvelu et al., 2003, Shen et al., 2009).

Because of this threat on the environment, it is required an effective way, to remove these dyes from the wastewater before discharge to the receiving water. This is an environmental challenge facing human society all over the world, since most of the dyes, are compounds that are chemically complex, and non-biodegradable (Lee et al., 2006).

Reactive dyes are widely used in many industries (Yagub et al., 2014) (e.g, rubber, printing, plastics, cosmetics, food processing industries etc.) especially in the textile for coloring their products (Bensalah et al., 2009, Dawood et al., 2014). There are more than 100000 types of industrial dyes as commercial, have a complex installation. In addition, synthetic dyes are very complex and are made to resist sweat, water and light. From these reason, the presence of reactive dyes in aquatic ecosystem causes major environmental problems on the earth (Aksu et al., 2008, Vijayaraghavan et al., 2008, Yagub et al., 2014).

Currently, environmental pollution considers the most serious problem facing the world (Paul et al., 2011). The existence of dyes in an aquatic ecosystem, reduces the penetration of light, so that prevents the process of photosynthetic activity.

Also, toxic compounds like reactive dyes cause a mutation (Carneiro et al., 2010), irritation, dermatitis and allergies, and poisoning in drinking water and changing the shape of water (Royer et al., 2010). So, dyes are considered as one of the most dangerous chemical items on human life (Royer et al., 2009).

Reactive dyes; are a significant group of industrial dyes because they have a covalent bond between its reactive groups and surface groups of textile and cellulose filament.

Presence of reactive dyes in an aquatic ecosystem is a danger to the environment as it is highly non-biodegradable, toxic and causes mutations (Asouhidou et al., 2009, Pearce et al., 2003). Furthermore, reactive dyes are unaffected by conventional treatment systems, because of the aromatic rings in its structure.
According to this feature reactive dyes are considered as the most problematic among other dyes (Lazaridis et al., 2003, Pearce et al., 2003). Among reactive dyes, Reactive Red-120 (RR-120) is one of the frequently used dyes in textile industries and is a potential threat to the aquatic environment due to its poor biodegradability (Çelekli et al., 2009; Paul et al., 2011).

1.2 Treatment Technologies of Dyes

In the last two decades the process of dye wastewater treatment has been studied (Adegoke et al., 2015). There are several reported treatment processes for the elimination of dyes from aquatic ecosystem. These technologies can be split into three categories: physical, chemical and biological methods (Adegoke et al., 2015).
However, the conventional treatment methods have advantages and disadvantages. The disadvantages are high expense and occurrence of disposal problems. Many of these traditional styles of treating dye wastewater have not been used at large scale in the paper and textile industries (Devi et al., 2008). At the present-day, no single treatment method has the ability to treat wastewater contaminated with dye due to the complex nature of these toxic compounds (Janos et al., 2005, Zhu et al., 2008).
Despite the availability of such styles to expel these pollutants of wastewater as lawful requirements, such as chemical oxidation, anaerobic microbial degradation,

coagulation, electrochemical, and aerobic and membrane separation process. These styles are not very successful to solve the problem (Sulak et al., 2008).

Among these processes, adsorption has been choosing due to its high-quality to remove hazardous dyes chiefly into well-designed sorption processes and cheapness (Çelekli et al., 2018). Adsorption by activated carbon is a substantial path to cleanup wastewater (Semerciöz et al., 2017). However, adsorption by activated carbon has some limitation like the cost of activated carbon, the lack of renewal after exhausting and the loss of adsorption qualification after the renovation (Srivastava et al., 2007).

1.2.1 Physical Treatments

1.2.1.1 Electro Kinetic Coagulation

Adding ferric chloride and ferrous sulfate, allows excellent removal of the dyes from the wastewater and considered as an economical and inexpensive way to remove dyes.

Unfortunately, due to high-cost of ferrous sulfate and ferric chloride, this method gives bad results with acid dyes and this means it is not a widely used method (Brillas et al., 2015). The disposal costs are high because this process involves the product of big amounts of clay (Brillas et al., 2015).

1.2.1.2 Ion Exchange

There is a scientific judgment that says ion interchanges can't ingest a wide domain of dyes. This is why ion exchange is not widely used to treat waste containing dye (Solís et al., 2012).

In this method wastewater is passed through the ion interchange resin to the ready truck sites are filled (Klavarioti et al., 2009).

1.2.1.3 Membrane Filtration

The most important ability to clarify and focus this technique has the characteristic of separating the dye continuously from the aquatic ecosystem. The advantages of this method are resistance to microbial attack, harmful chemical environment and resistance to temperature. One of the disadvantages is the high cost and the replacement of membranes used in the removal process. (Solís et al., 2012).

1.2.1.4 Activated Carbon

Adsorption is the most common method to remove dyes (Pérez et al., 2012) and it is considered highly effective to sorbing vat, cationic, and acid dyes while in a little lesser range, reactive dyes, pigment, mordant, direct and dispersed. The quality of the reaction depends on the characteristics of the wastewater and the type of carbon used. (Klavarioti et al., 2009).

1.2.1.5 Irradiation

There is a need for enough quantity of dissolved oxygen. This solved oxygen is wasted so quickly, thus it is necessary to provide an adequate amount of it, this has an impact on cost. Using a dual-tube bubbles manager can treat waste containing a dye as some pigments and phenolic molecules can be oxidized effectively on a laboratory scale only through this method (Pérez et al., 2012).

1.2.2 Chemical Methods

1.2.2.1 Sodium Hypochlorite (NaOCl)

The amino acid constituents of dye molecules in this process are attacked by Cl, and accelerates the division of azo bond. In this process, when the concentration of Cl increases, the removal of the dye increases. Because of the negative effect of Cl release in the waterways, the use of chlorine to remove the dye has become less frequent (Manjarrez et al., 2012), liberation toxic molecules, or the release of aromatic amines which are carcinogenic (Flores et al., 2012).

1.2.2.2 Oxidative Processes

The basis for the simplicity of this process, is to make it the most widely used chemical removal method. The main oxidant factor in this process is hydrogen peroxide (Flores et al., 2012). As result of the fragmentation of the aromatic ring of dye molecules in this method the dye is removed from the waste by oxidation (Pérez et al., 2012).

1.2.2.3 H2O2±Fe (II) Salts (Fentons reagent)

Fentons reagents are used as a chemical method of treatment wastewaters (Manjarrez et al., 2012). It may be shown to be effective in removing the color from both soluble and insoluble dyes. Bonding to remove dissolved dyes from wastewater is the cornerstone of this chemical separation process (Klavarioti et al., 2009).

1.2.2.4 Ozonation

The use of ozone was first initiated in the premature 1970s (Brillas et al., 2015). The tested dose of effluents containing dyes depends on the total color and the lagging COD that needs to be removed with no sludge residue and no metabolic poison. Because it does not increase the sludge and the volume of wastewater, it is the main feature that ozone ability exists used in its gassy case (Brillas et al., 2015).

1.2.3 Biological Treatments

1.2.3.1 Decolourisation via Blank-Mold Fungi

The structural polymer found in wooden plants, white-rot fungi are those organisms that are capable of degrading lignin (Manjarrez et al., 2012). That fungus are able to insult polychlorinated biphenyls (PCBs), dioxins while another chloro-organics (Pérez et al., 2012). Have a display that *Phanerochaete chrysosporium* had the ability to decolorized synthetic textile torrential via up to 99% in 7 days.

1.2.3.2 Other Microbial Cultures

A mixture of dyes, has been removed in 24-30 hours, by the use of anaerobic bacteria. Growing free cells or various supporting substances in the form of biofilms (Flores et al., 2012). As well as the use of bacteria for the biodegradation of azo dye. However, this system is unable to deal with large amounts of textile effluents, this makes its apparent disadvantage is its need for fermentation processes.

In aerobic conditions, azo dyes cannot be metabolized although some *Pseudomonas* strains may be able to analyze some azo dyes (Flores et al., 2012).

The capacity of some bacteria to metabolize azo dyes was determined via research groups in 15 days, the mixed bacterial cultures from a wide set of habitats have else been shown to decolorize the diazo linked chromophore of dye molecules (Flores et al., 2012).

1.2.3.3 Sorption via Living/Dead Microbial Biomass

Textile dyes varied in their chemical structures, and thus their interactions with microorganisms rely on the specific chemistry of the microbial biomass and the chemistry of a particular dye (Pérez et al., 2012). Depending on the types of micro-organism and the dye utilize different bound averages while abilities will exist spotted.

It able exist told these confirmed dyes to own a special alliance to binding to microbial types. The uptake or accumulation of chemicals by microbial mass has been describing bio sorption (Solís et al., 2012). Fungi, yeast and Dead bacteria have all been used for the aim of decolorizing dye-containing effluents. Sorption via biomass takes place via ion interchange. (Solís et al., 2012).

1.3 *Moringa Oleifera*

The nomenclature of this plant is given as

Kingdom : - Plantae

Subkingdom : - Viridiplantae

Infrakingdom : - Streptophyta

Superdivision : - Embryophyta

Division : - Tracheophyta

Subdivision : - Spermatophytina

Class : - Magnoliopsida

Superorder : - Rosanae

Order : - Brassicales

Family : - Moringaceae

Genus : - *Moringa*

Species : - *Moringa oleifera* Lam.

M. oleifera, a 12 m long tree, grows rapidly in arid tropics. As well as living in sandy or poor soil near the coasts (Falowo et al., 2018). It exists in South America, the Caribbean, the Pacific, Southeast Asia and the Arabian Peninsula is currently growing in many regions including Africa and living in the northern India (Falowo et al., 2018). They are cultivated for their medicinal value and the use of their leaves and seeds in cooking for their nutritional benefits.

The most famous of this tree applied in the field of water purification turbidity was all scientific research focused on this aspect. As an alternative to aluminum sulfate proved to be effective in the treatment of water because the seeds of different types of them contain cationic polyelectrolytes.

M. oleifera seeds possess antimicrobial properties, remove turbidity, and do not affect pH in water, low sludge volume, and production of biodegradable sludge. For these reasons *M. oleifera* success in the field of purification of polluted water, whether industrial or turbid water of a river or marine nature (Abu-Bakr et al., 2017). The mechanism by which seeds work on microorganisms is not fully understood. However, *M. oleifera* tissue was analyzed from a wide range of sources of glucosinolates and phenols (anthocyanins, flavonoids, and branthocyanidines). Seeds of *M. oleifera* are reported to be 4- (α-L-Ramanopiranosyloxy) -benzylglucosinolate in high concentrations.

1.4 Aim of Study

In the present study, the main purpose was to use eco-friendly an alternative adsorbent from *Moringa oleifera* seed, which has also elimination problem, to remove Reactive Red 120 (RR120). While this processes, making better quality with energy and time saving is considered by using adsorption technique. In this way, *M. oleifera* which is known as miracle tree because of its chemical and porous structure is evaluated as adsorbent and dyes contaminated wastewater is regained.

Aims of this study were;

- To explore the adsorptive potential of a new adsorbent from *M. oleifera* (MO) seed for removing of RR 120 from aqueous solutions as functions of type of MO, particle size of MO, solution pH, adsorbent value, contact time (kinetic studies at various temperatures).
- To evaluate initial RR 120 concentration (isotherm studies at various temperatures were evaluated to obtain the thermodynamic parameters).
- To characterize the MO by determinations of FTIR, SEM and pHzpc analyses, and to obtain eco-friendly alternative adsorbent for removing RR 120 and to save energy and time.

CHAPTER II
LITERATURE REVIEW

2.1 Literature review of *Moringa oleifera*

Here, are some of the previous studies about *Moringa* tree generally, then followed studies about its seeds in special. To clarify their impact on all the experiments used:

Kumari (2005), researched that *M. oleifera* seeds powder was used for arsenic removal from water, under the optimal conditions. *M. oleifera* seeds powder achieved sorption of 60% for trivalent arsenic, and 86% for pentavalent arsenic.

Katayon (2006), looked into the preservation of *M. oleifera* seeds coagulation efficiency. It is found that *M. oleifera* is coagulating components are highly biodegradable resulting in very short shelf life. They stored seeds powder in closed containers at 4¼ Celsius, and stored freeze-dried seed powder in closed containers and vacuum packs. The (non-freeze-dried) powder, refrigerated in a closed container maintained its coagulation efficiency above 80% for 10 months. The (freeze-drying) seeds powder preserves its coagulation efficiency, regardless the effect of temperature and packaging method.

Oluduro and Aderiye (2007), used a crude extract from dried seed powder of *M. oleifera* to sought to discover its seeds effectiveness in reducing bacteria and coliforms in raw water. They reported that, 90% total bacteria and 99% total coliforms had been precipitated from the water sample after 24 hours of treatment. Using a specific concentration of the extract, no microbial growth occurred in the treated water samples after being stored for 96 hours.

In addition to *M. oleifera* seeds several promising plant extracts such as *Jatropha curcas* and *Guar gum* extracts have the ability to decontaminate water from shallow wells (Pritchard et al., 2009). Optimal water purification dosages for *J. curcas* and *G. gum*, were discovered to be 50 mg/L. While *M. oleifera* seeds optimal dosage was discovered to be 250 mg/L. Though the optimal dosage was five times higher for *M.*

oleifera seeds than for the other plant extracts. *M. oleifera* seeds, produced the best results in reducing water turbidity, removing 100% of turbidity.

Lea (2010), offered additional practical advice regarding *M. oleifera* seeds utilization. The author, found that *M. oleifera* trees mature quickly, producing seeds within their first year. The extraordinary seeds are not only excellent water purifiers; they also contain a high-quality food oil called Ben oil. Besides he explains that the press cake remaining after oil extraction retains its ability to treat turbid water without diminished efficacy. This means that producers may obtain both valuable food oil and powder for water purification. The study points out that others have claimed *M. oleifera* seed is somewhat toxic; however the author found that the toxicity is not a concern at the low dosage levels used for water purification.

M. oleifera seeds, are effective against waterborne diseases; especially cholera, typhoid, and Escherichia coli (Atieno et al., 2011). The study employing methanol extract of *M. oleifera* seed; found that all three of these bacteria were inhibited to a degree by the extracts antimicrobial and antibacterial properties.

M. oleifera wood, a solid waste was used for the preparation of activated carbon for the removal of nickel, zinc, and copper from synthetic wastewaters. Effects of various operating variables namely solution pH, contact time, carbon dose, adsorbate concentration and temperature on the removal of metal ions have been studied (Kalavathy et al., 2010).

CHAPTER III
MATERIALS AND METHODS

3.1 Preparation of Adsorbent

Moringa oleifera (MO) was acquired from a field product of a company. A composed sample was washed twice with tap water. Dried seeds were then ground in a mortar, sieved via the use of different mesh sizes of sieves (<125, 125–250 and >250 μm), and stocked in airtight polyethylene bottles to furthermore studies. No chemical treating was utilized before to adsorption tests.

3.2 Preparation of Adsorbate

A stock dye solution (1 g /L^{-1}) was readied together a gram dye power with distilled water. Reactive Red 120 (RR 120), a reactive diazo dye, was acquired from Sigma (Sigma–Aldrich Chemical Co., St. Louis, USA). Experimental dye solutions were prepared by diluting stock dye solution with distilled water. The chemical structure (Figure 3.1) and ownership of that dye are presented in Table 3.1.

Table 3.1 General Characteristics of Reactive Red 120

Name of dye	**Procion Red HE-3B**
Colour index name	Reactive Red-120
Chemical formula	C44H24Cl2N14O20S6Na6
Molar mass	1,469.98 g/ mol^{-1}
CAS number	61951-82-4
λ_{max}	515 nm

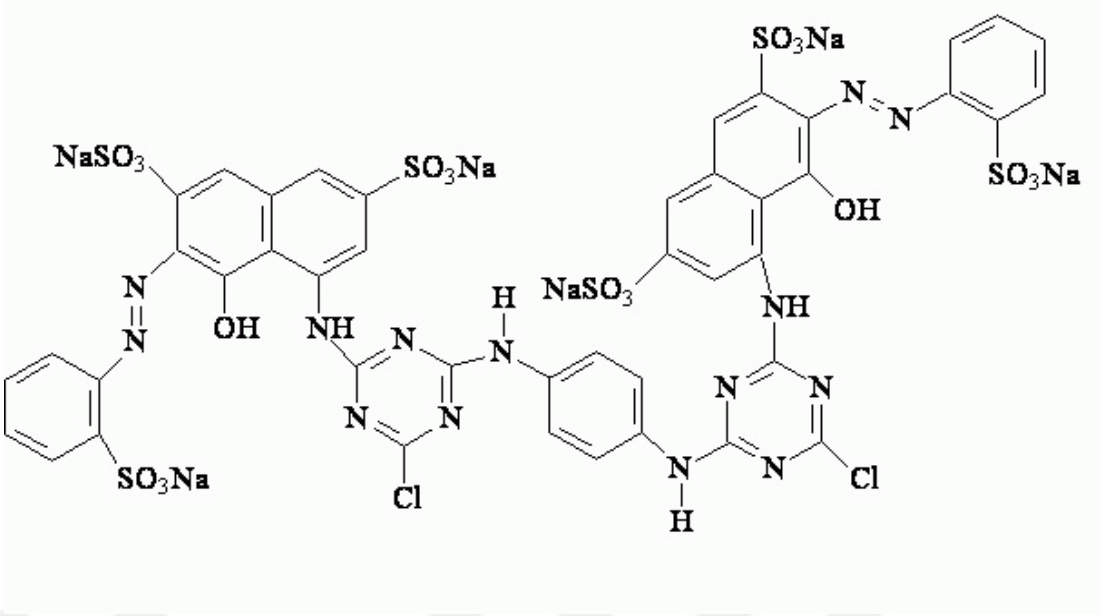

Figure 3.1 Chemical Structure of Reactive Red 120

3.3 Characterization of Adsorbent

3.3.1 FTIR–ATR Analysis

Fourier converts infrared radiation equipped with a reduced overall reversal spectrometer was applied (Perkin-Elmer Spectrum 100 FTIR–ATR Spectrometer), to describe *M. olifera* (MO) exterior structure before and after the sorption of RR 120.

3.3.2 Determination of pH Zero-Point Charge (pHzpc) of MO

A chain of mixture solutions (0.5 g adsorbent and 50 mL 0.1 M NaCl), at initial pH values ranging from (pH 1 to 9) in 100 mL conic flask were intended. Solution pH were adjusted with 0.1 M HCl and/or 1.0 M NaOH solutions. Batches were agitated on an orbital shaker at 150 rpm for 24 h and the definitive pH (pHf) was metrical at equilibrium. Value of zero-point charge was specified of the plot of (pH final) versus (pH initial). The pH_{zpc} of MO was specified by employ from powder extension method.

3.3.3 Scanning Electron Microscope (SEM) Analysis

The surface morphologies of MO samples were studied using the scanning electron microscope (SEM) system (JUL-6390 LV). For the purpose of the assay, the adsorbent samples were prepared in a variety of ways. For the purpose of the examination, the adsorption samples were raw and RR120 loaded MO seeds.

3.4 Absorption Study

The pH of adsorption solutions was regulated to required values with 0.1 M KOH or/and 1.0 M HCl. Tests were completed with 100 ml of sorption solutions together with required dye concentricity and adsorbent dose at destined pH in value 250 ml conic flasks. The conical flasks were agitated on an orbital shaker at 150 rpm for the ample time. Impacts of initial pH values (pH 1–9), particle size (<125, 125–250 and >250 μm), (contact time (0–100 min), adsorbent dose (0.5, 1.0, 2.0, and 4.0 mg/L), initial dye concentrations (10, 20, 40, 60, 80, and 100 mg/L) and temperature (293, 303, 313, and 323 K). were elaborated under the sides of sorption kinetics, thermodynamic, activation energy and desorption studies.

A sample solution was regulated with wanting dye at the selfsame case and its presenting color to a solution was specified by use of spectrophotometer. It was found that it gave so small (trivial) color to a solution. Specimens were isolated at 0, 15, 30, 45, 60 and 90 min and centrifuged at 6000 x g for the 5 min. The lagging RR 120 concentricity in the supernatant was read absorbance by a spectrophotometer (Jenway 6305) at 515 nm. Any datum spot was the mean of two separate adsorption studies. Values of q_t and q_e are neutralized of RR 120 adsorbed on MO at time t (mg g-1), studied via employ of (Eq.3.1) and (Eq.3.2).

In order to obtain the q_t values, samples were taken from experiment sets with a time interval as above and their RR120 concentrations were analyzed with a (UV/Vis Spectrophotometer (Jenway 6305)). Data from was used to calculate q_t values by Equation 3.1.

$$q_t = \frac{(C_0 - C_t) * V}{m} \tag{3.1}$$

$$q_e = \frac{(C_0 - C_e) * V}{m} \tag{3.2}$$

Where C_0 and C_t represent remain dye concentrations (mg/L) at initial and at t time, respectively. V is the volume of solution (L), and m is adsorbent mass (g /L).

3.5 Sorption Kinetic Modeling

In order to investigate the adsorption kinetics of RR120 on MO seeds, the utmost generally utilized kinetic models; (pseudo second-order kinetic (Eq.3.3), Avrami

(Eq.3.4), logistic (Eq.3.5) and Elovich (Eq.3.6)) are given in table 3.2. Were utilized to experiential datum.

Table 3.2 Equations of Kinetic Models

Kinetic Models	Equations	References
Pseudo-second order	$\frac{t}{q_t} = \frac{1}{k * q_e^2} + \frac{t}{q_e}$	Ho and Mckay, 1995
Logistic	$q_t = \frac{A}{1 + (\frac{t}{b})^c}$	Çelekli et al., 2010
Avrami	$q_t = q_{epred}\ \{1 - \exp[-(K_{av}\, t)]^{n_{av}}$	Avrami, 1939
Elovich	$qt = \frac{1}{\beta} * (\ln(1 + (\alpha * \beta * t)))$	Plazinski et al., 2009

3.6 Equilibrium Models

Freundlich (Eq.3.7), Langmuir (Eq.3.8), Temkin (Eq.3.9), and Dubinin-Radushkevich (Eq.3.10) isotherms (Table 3.3) were used to characterize the relation between adsorbed RR120 per unit mass of MO (qeq; mg/g) and unabsorbed dye values in the solution (Ceq; mg/L) at the equilibrium.

Table 3.3 Equations of Equilibrium Models

Models	Equation	Reference
Freundlich	$\log q_e = \log K_f + \frac{1}{n} * \log C_e$	Freundlich 1907
Langmuir	$\frac{C_e}{q_e} = \frac{1}{q_L * K_L} + \frac{C_e}{q_L}$ $R_L = \frac{1}{1 + (K_L * C_o)}$	Langmuir 1918
Temkin	$qe = \frac{RT}{bt} \ln At + \left(\frac{RT}{bt}\right) \ln Ce$	Temkin,

		Pyzhev 1940
Dubinin-Raduskevish	$\ln q_e = \ln q_m - \beta\varepsilon^2$ $\varepsilon = R * T * \ln(1 + \frac{1}{C_e})$	Dubinin, Radushkevich 1947

3.7 Thermodynamic Studies

Thermodynamic studies were performed at four different temperature values (293, 303, 313, and 323 K). From (Eq.3.11) Gibbs free energy change values, ΔG°, were calculated by using of K_L constant from Langmuir model. Other variables, entropy change, ΔS°, and enthalpy change, ΔH°, were calculated from ΔG° versus T (K) plot bases (Eq.3.12).

$$\Delta G° = RT\ln(K_L) \tag{3.11}$$

$$\Delta G° = \Delta H° - T\Delta S° \tag{3.12}$$

Where R (8.314 J mol^{-1} K) is the universal gas constant. The slope and intercept of a plot (not shown) of 1/T (temperature, K) against $\ln K_L$ was used to determine values of ΔH° (kJ mol^{-1}) and ΔS° (J mol^{-1} K^{-1}).

3.8 Validation of Models

Fitting of findings was estimated by using the mercantile computer software Sigma Plot version 11 (Systat Sofware, Inc., California, USA) by the Marquardt–Levenberg algorithm. On the other hand, q predicted (q_{pred}) values and constants of three equations were obtained with this algorithm. So as to estimate the interest from suitable; correlation coefficients (R^2), the sum of squares errors (SSE) was executed amidst experiential and prophesy datum (Çelekli et al., 2010).

$$SEE = \sqrt{\frac{\sum(q_{exp} - q_{predict})^2}{N}} \tag{3.13}$$

CHAPTER IV
RESULTS AND DISCUSSION

4.1 Adsorbent Characterization

4.1.1 FTIR Analysis

All adsorbents have various obligating capability for the removal of dye molecules. Sorption capability is not only impacted by the porous structure or textural of sorbents, but is also hardly affected by the chemical structures of the exterior. The part of MO exterior consist of various proteins, lipid, and polysaccharides containing different effective groups like carboxyl, carbonyl, amino, hydroxyl, phosphate, sulphonate, and sulphydryl, whose ability rule as obligating locations to dye molecules. FTIR-ATR technique was used to discover changes in the surface of adsorbent FTIR-ATR spectra of natural and MO mix before and after the sorption of RR 120 are shown in (Fig 4.1) and the result present in (Table 4.1).

Functional groups on the surface of the MO responsible for RR 120 adsorption were characterized by FTIR-ATR. Three different adsorbent FTIR-ATR analyzes were performed to determine the surface shell, inner, and scratches of the MO seeds.

The results of natural, pre- and post-RR 120 removal on the MO mixed seed at pH1 are shown in Table 4.1 and Figure 4.1a, b and c, respectively, in the natural structure of the MO seed mixture; 3285, 2922, 1745, 1648, 1539, 1456, 1231, 1160 and 1096 significant bands were observed in the 1 / cm wave number. The relevant functional group for each band is given in Table 4.1. For example, the peak at 3285 1 / cm indicates the groups -OH and -NH2 (Arief et al., 2008; Mahmoodi et al., 2010, Celekli et al., 2011). Methyl and methylene groups show the presence of the carboxyl group at 1729 1 / cm at 2922 1 / cm (Çelekli et al., 2009; Yang and Qui, 2010, Arief et al., 2008). The bands at 1232 and 1032 1 / cm show the C-O groups (Arief et al., 2008, Çelekli et al., 2009).

Table 4.1 MO Seeds Mixture Adsorbent pH 1, Natural, Before and After removal of RR 120 dye.

		pH 1	
Groups	**Natural**	**before**	**after**
-O-H –NH2	3285	3333	3287
-CH_3	2922	2922	2922
Karboksil	1745	1745	1745
C-O	1648	1648	1645
Amid II	1539	1540	1540
-N-H	1456	1457	1457
-SO3	1231	1231	1229
C-O-C, P=O	1160	1153	1159
P-O, C-C, COO-, C=O	1096	1096	1095

The mixture of MO seeds differed only slightly in some bands after the natural adsorbent was stored at pH 1 in the water solution only (Table 4.1). Significant changes were observed in the mixed surface structures of MO before and after RR 120 adsorption (Table 4.1 and Figures 4.1a-c). Bands such as 3287, 2922, 1745, 1645, 1540, 1457, 1229, 1159 and 1095 1/cm were observed after adsorption. Table 4.1. and figures 4.1a-c indicate that some of the bands present on the adsorbent after adsorption are unchanged, some change and new bands appear. This shows that RR 120 was adsorbed on the adsorbent. Similar results have been reported for the RR 120 adsorption on *Lentinus sajor-caju* (Arica and Bayramoğlu, 2007), *Spirogyra majuscula* (Çelekli et al., 2009), peanut shell (Çelekli et al., 2010), and *Hydrilla verticillata* (Çelekli et al., 2012b). Amino acid, carbonyl, and amide groups on the adsorbent played significant roles the sorption of RR 120 the MO seed mixture.

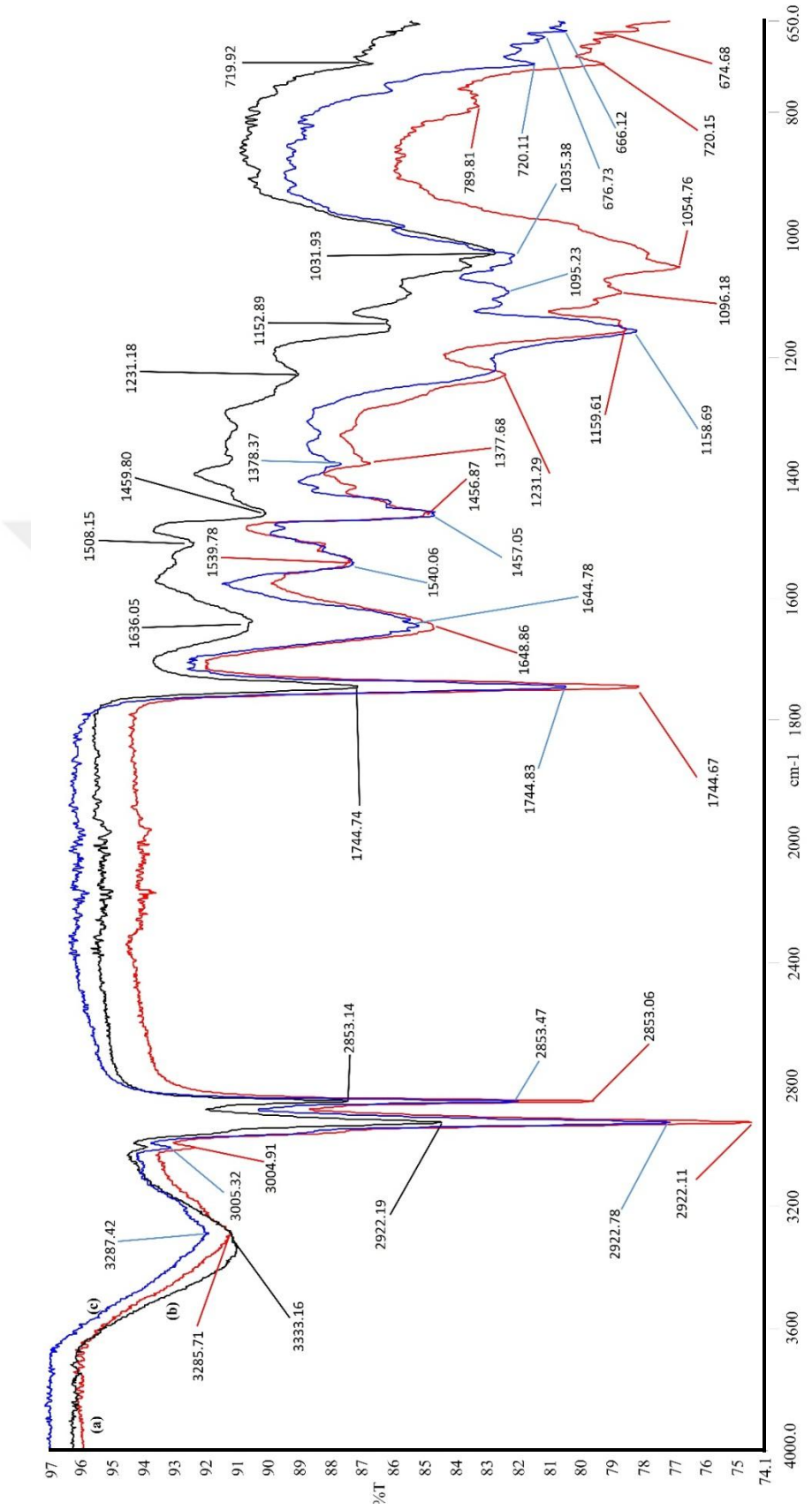

Figure 4.1 The MO seed mixture; (a) natural and at pH 1, (b) before and (c) after the adsorption of RR 120.

The results are shown in Fig. 4.2a, b, c and Table 4.2 respectively, before and after RR 120 dye removal at pH 1, natural seed adsorbent. In the natural structure of MO plain seed adsorbent; 3287, 2923, 1745, 1649, 1544, 1457, 1378, 1232, 1159 and 1054 significant bands were observed in the 1 / cm wave number. The relevant functional group for each band is given in Table 4.2.

Table 4.2 MO inner seeds adsorbent, natural, before and after Removal of RR 120 dye at pH1.

		pH 1	
Groups	**natural**	**before**	**after**
-O-H –NH2	3287	3342	3287
-CH_3	2923	2924	2923
Karboksil	1745	1745	1745
C-O	1649	1648	1645
Amid II	1544	1545	1544
-N-H	1457	1435	1458
	1378	1337	1328
-SO3	1232	1230	-
C-O-C, P=O	1159	1144	1160
P-O, C-C, COO-, C=O	1054	1060	1037

MO inner seed natural adsorbent only differed in some bands after standing at pH 1 in water solution (Table 4.2). Significant changes were observed in the mixed surface structures of MO before and after RR 120 adsorption (Table 4.2 and Figures 4.2a-c). Bands such as 3287, 2923, 1745, 1645, 1544, 1458, 1328, 1160 and 1037 1 / cm were observed after adsorption. Some of the bands present on the adsorbent after adsorption, as evidenced in Table 4.2 and Figures 4.2 b, c, were unchanged, some changed, and new bands appeared, which indicates the sorption of RR 120 on the adsorbent. Functional groups of MO such as amino, carbonyl and amide play a important roles on the removal of RR 120.

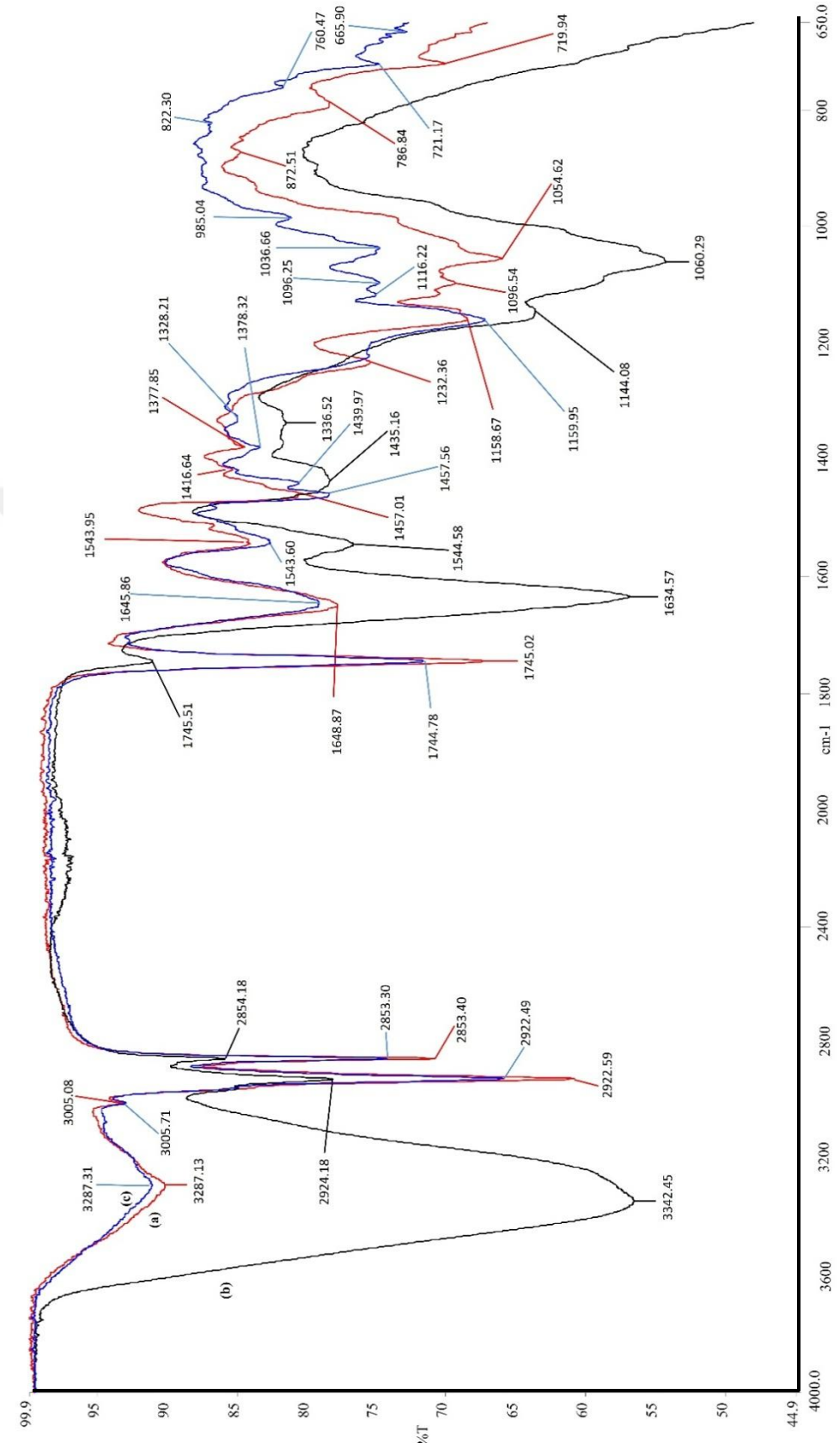

Figure 4.2 The MO inner seeds; (a) natural and (b) before and (c) after the adsorption of RR 120 at pH1.

The results of natural, before and after RR 120 dye removal at pH1 on the MO seed are given in Figures 4.3a, b, c and Table 4.3 respectively. In the natural structure of the shell adsorbent of MO seeds; 3287, 2922, 1740, 1635, 1509, 1419, 1308, 1231, 1150 and 1028 1 / cm wave number. The relevant functional groups for each bands are given in Table 4.3.

MO inner seeds adsorbent natural, before and after removal of RR 120 dye at pH1.

Table 4.3 MO seeds shell; natural, before and after removal of RR 120 dye at pH1.

		pH 1	
Groups	**natural**	**before**	**after**
-O-H –NH2	3287	3286	3291
-CH_3	2922	2910	2925
Karboksil	1740	1730	1746
C-O	1635	1636	1637
Amid II	1509	1509	1508
-N-H	1419	1426	1437
	1308	1320	1329
-SO3	1231	1232	1222
C-O-C, P=O	1150	1148	1156
P-O, C-C, COO-, C=O	1028	1028	1037

MO seed shells having different bands only after the natural adsorbent was stored at pH 1 in the water solution (Table 4.3). Significant changes were observed in the mixed surface structures of this adsorbent before and after RR 120 adsorption (Table 4.3 and Figures 4.3a-c). Bands such as 3291, 2925, 1746, 1637, 1508, 1437, 1329, 1222, 1156 and 1037 1 / cm were observed after adsorption. As is clearly seen in Table 3.3 and Figures 4.3b, c, some of the bands present on the adsorbent after adsorption were unchanged, some changed and new bands appeared. Changed and appeared new bands could be due to the binding of RR 120 on the adsorbent. Functional groups of MO such as amino, carbonyl and amide groups were responsible for the removal of RR 120.

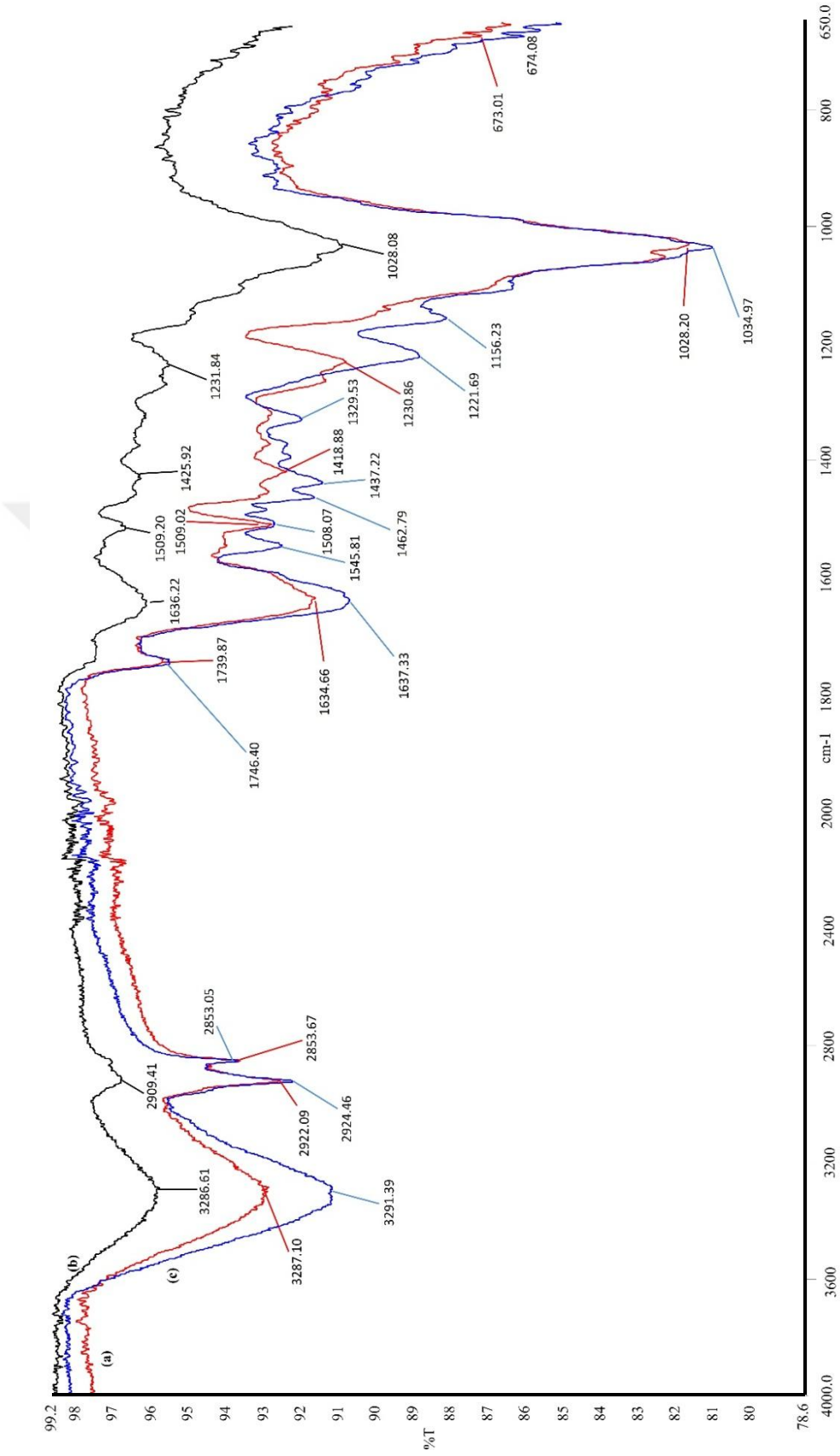

Figure 4.3 The Removal of The RR 120 at pH 1, a Natural, b Before and c After the Adsorption of the MO Shells.

4.1.2 SEM Analysis

Scanning electron microscopy (SEM) images of surface and pores before and after the RR 120 removal with MO seed are given in Figures 4.4a and b, respectively. Differences between superficial morphologies of different biomass species studied are shown in SEM form. In the natural appearance of the dried MO shell (Fig. 4.4a) no breakage was observed and numerous pores were seen. After the RR 120 removal, it is thought that the pores in the surface of the adsorbent have been shrunk so that they could play an important role on the adsorption capacity (Figure 4.4b). These changes in the surface of the adsorbent can be attributed to the use of different agricultural wastes such as apple wastes (Hesas et al., 2013), orange peel (Fernandez et al., 2015) and pumpkin husk (Çelekli vd., 2018) have also been reported in previous adsorption studies.

(a)

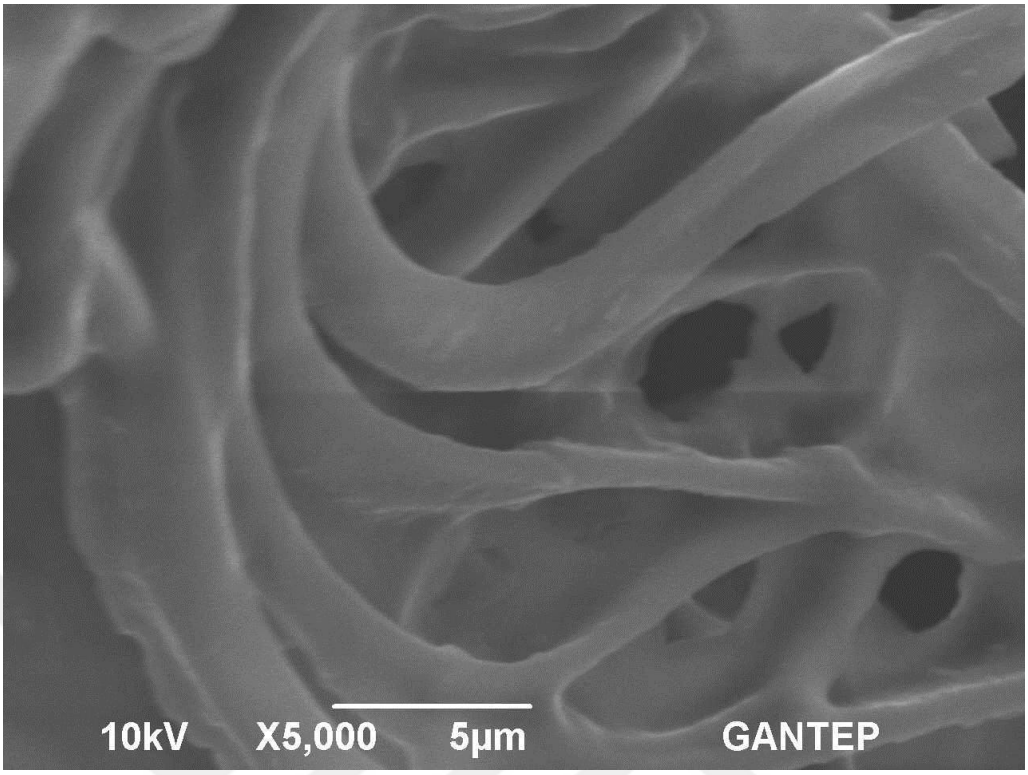

(b)

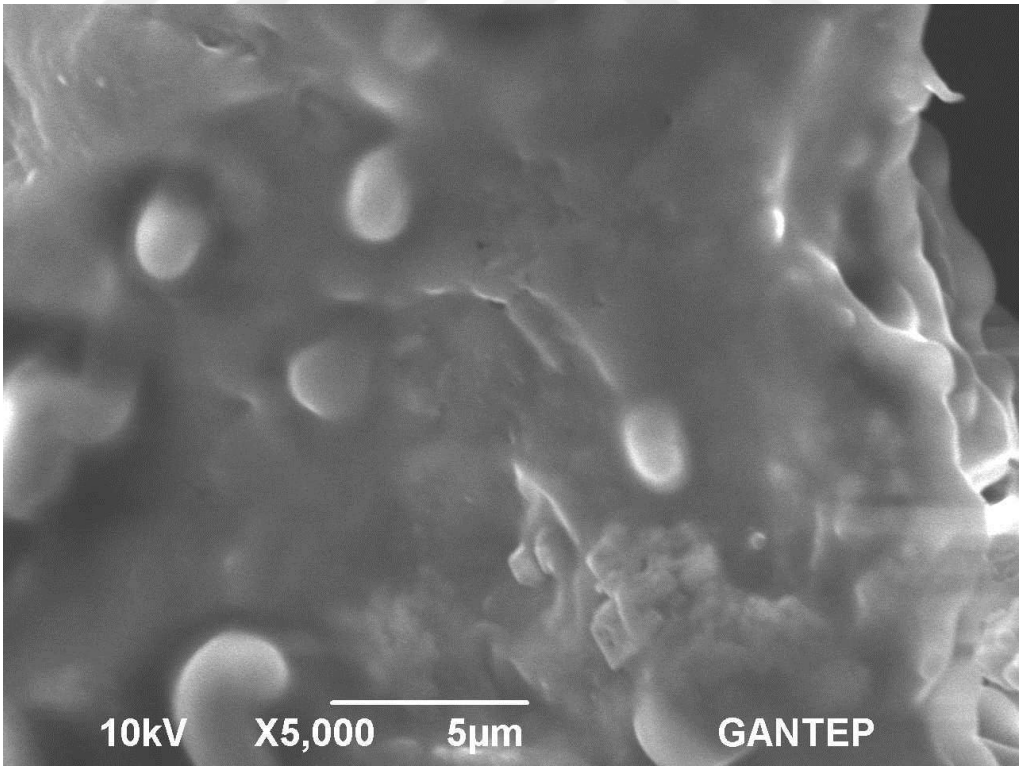

Figure 4.4 MO seed (a) before and (b) after the RR 120 sorption.

4.1.3 Effect of pHzpc

Determination of adsorbent pH zero load point (pH_{zpc}) (zero point charge, pH_{zpc}) is crutial to understand the adsorption mechanism. The pH_{zpc} of each part of the MO seed was determined separately. Results of the study were determined as internal seed pH_{zpc} 4.4 (Fig. 4.5), seed shell pH_{zpc} 5.2 (Fig. 4.6) and seed mixture pH_{zpc} 4.5 (Fig. 4.7). The results of the present study showed that the MO seed sections differed slightly in pH_{zpc} because they contained different ionic groups. When the initial pH of the sorption solution is lower than pH_{zpc}, the adsorbent proton is loaded. It will support the adsorption of anionic dyes due to the increased electrostatic attraction. When solution $pH>pH_{zpc}$, adsorption of anionic dyes is limited due to increase of electrostatic repulsion force (Kumar et al., 2010, Naven et al., 2010, Cardoso et al., 2011, Celekli et al., 2011).

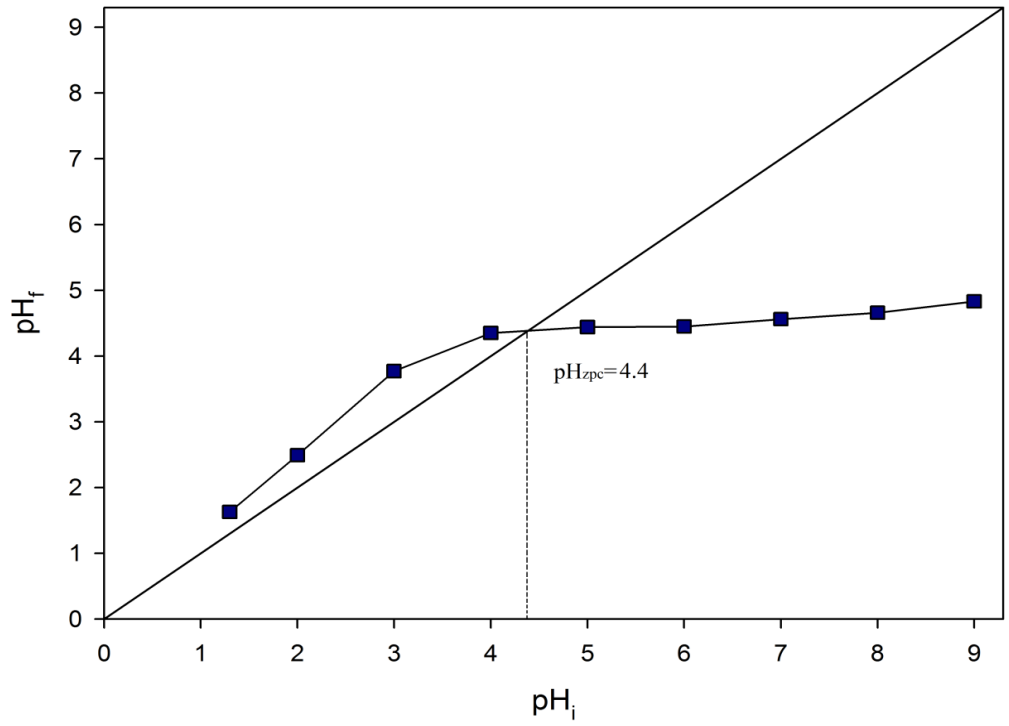

Figure 4.5 The pH_{zpc} of MO seeds.

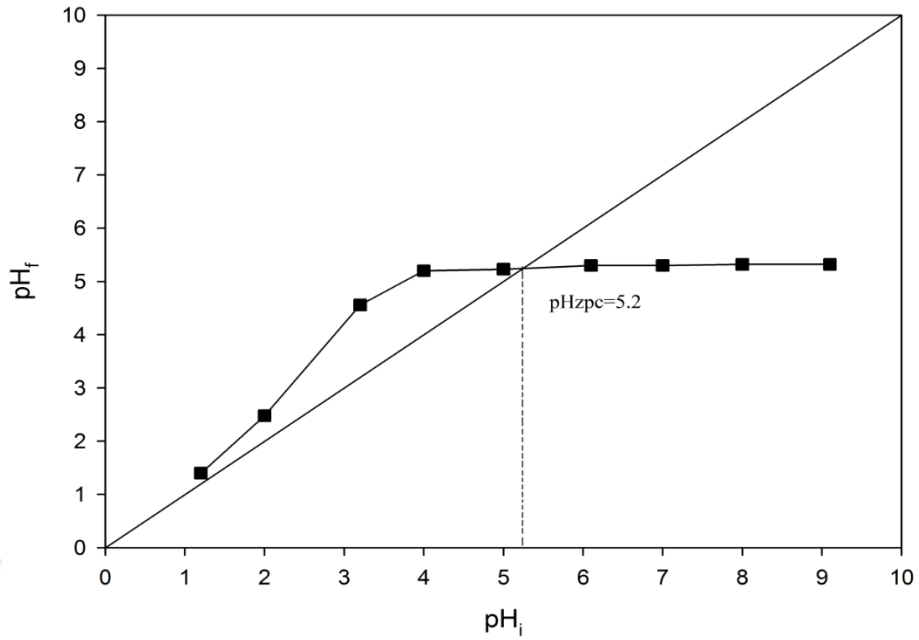

Figure 4.6 The pH_{zpc} of MO shell.

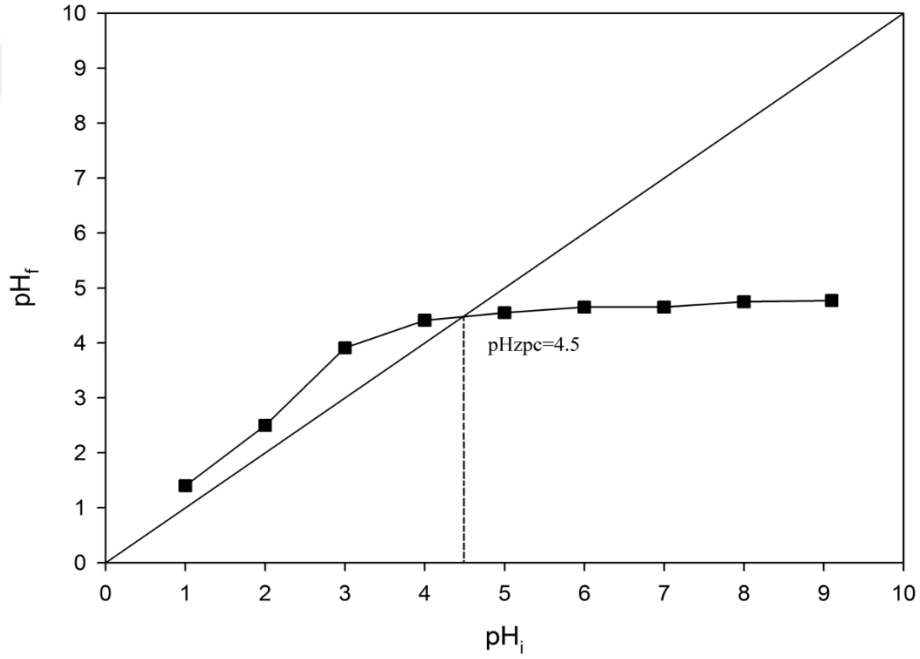

Figure 4.7 The pH_{zpc} of MO seed mix.

4.2 Absorption Study

4.2.1 Effect of Initial Solution pH

In sorption studies, pH is an important environmental factor. The initial pH of the solutes does not only play a role in the change of charged groups on the adsorbent, but also affects both the chemistry of the dye in the solution and its decomposition. In addition, oxidation-reduction potential also affects the properties of solutions such as precipitation and hydrolysis. For this reason, the pH level only affects the sorption capacity of the adsorbent at the same time as it does not only change the customization of the dyes and their adsorption capacities (Aravindhan et al., 2007, Çelekli et al., 2010a). The pH_{zpc} of adsorbent is an important element for understanding the mechanism of adsorption. Results of the present study showed that the pH_{zpc} of MO varied between 4.4 and 5.2 (Figure 4.5-4.7). Due to the increase in electrostatic attraction force, it will support the adsorption of anionic dyes such as RR 120. When solution pH > pHzpc, adsorption of anionic dyes is limited due to increase in electrostatic repulsion. Change in pH values strongly affected ($p<0.01$) the adsorption of RR 120 and increasing initial pH value decreased the amount of adsorbed dye at the equilibrium state (Fig. 4.8), in agreement with findings of previous studies (Naven et al., 2010; Cardoso et al., 2011, Çelekli et al., 2011) In subsequent runs the adsorption solutions were adjusted to pH 1.

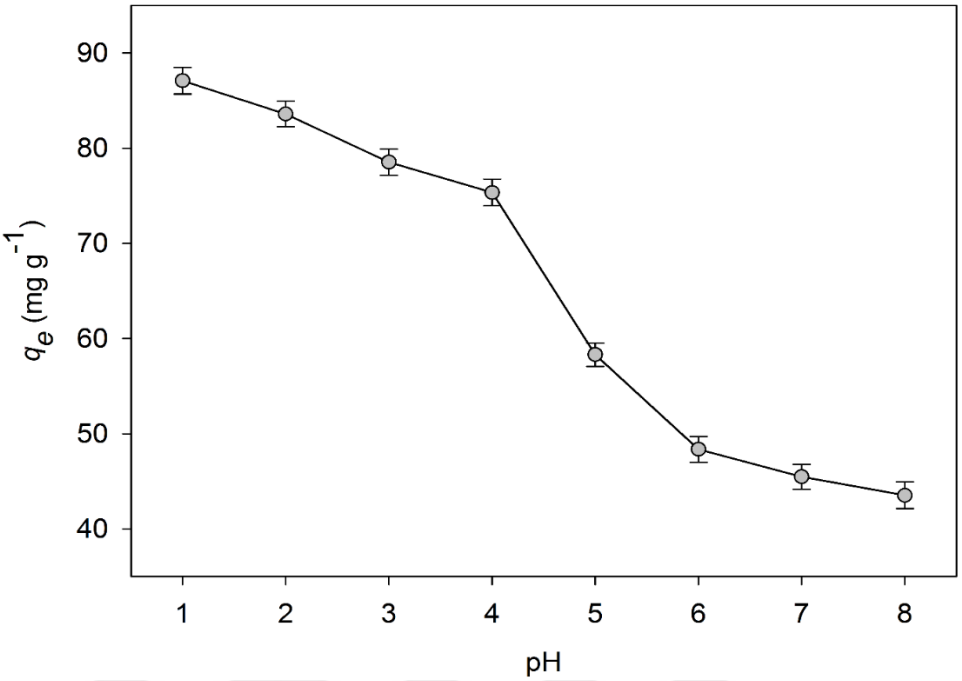

Figure 4.8 Effect of Initial pH Values on The Sorption of RR120 on MO Mix.

4.2.2 Effect of MO Type

The sorption of RR 120 on the shell, inner, and mix of MO seed were executed at different contact times (t = 0–100 min) at 50g/ L RR120 and 293 K beneath the pH = 1. The relations between MO types and their adsorption values are plotted in Fig. 4.9. The maximum sorption of RR120 was found on the MO mix, followed by MO inner seed and the minimum sorption was found on the MO seed shell. MO seed mix had great capacity for the adsorption of RR 120. This could be due to the increased absorption area and synergy effect with together parts of MO seed. Thus, MO seed mix as an adsorbent was chosen for the furthermore sorption studies.

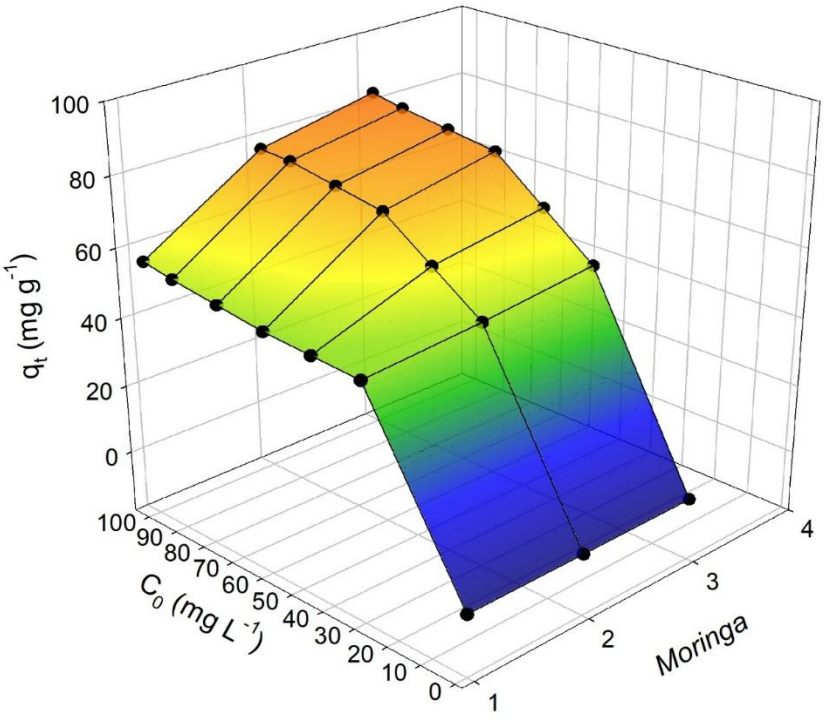

Figure 4.9 The effects of the MO seed parts (shell (1), inner seed (2), mixture (3)) on RR 120 adsorption (pH 1, C_0 = 50 mg / L and 293 K).

4.2.3 Effects of Particle Size

Particle size of adsorbent in adsorption studies is one of the important factors affecting the sorption capacity. The effect of the particle sizes (<125, 125-250 and >250 μm) on the adsorption process of 50 mg / L RR 120 was studied at pH1. The effect of the particle size of the MO seed mix on the sorption of RR 120 is shown in Figure 3.10. The adsorption capacity of MO increased from 78.40 mg / g to 85.86 mg / g when the particle size was reduced from >250 μm to <125 μm. There was a statistically significant difference ($p < 0.01$) between MO adsorbents RR 120 removal rates with different particle sizes. The conversion of the adsorbent into small particles causes both the increase of the surface area of the adsorbent and the easier penetration of the dye molecules into the adsorbent pores (Çelekli et al., 2011). With increasing surface area of the MO having small particle size, the amount of functional groups responsible for adsorption has also increased. Appearance of functional groups increased with decreasing small particle size, enhanced the

sorption capacity. Similar results have been reported in the sorption of bamboo with Blue 5G (Fiorentin et al., 2010), coconut shell (Gupta et al., 2010) and walnut shell with Lanaset Red G (Çelekli et al., 2012). Maximum sorption of RR 120 on the MO seed mixture occurred at<125 µm particle size. For this reason, adsorbent with the smallest particle size was used in subsequent studies.

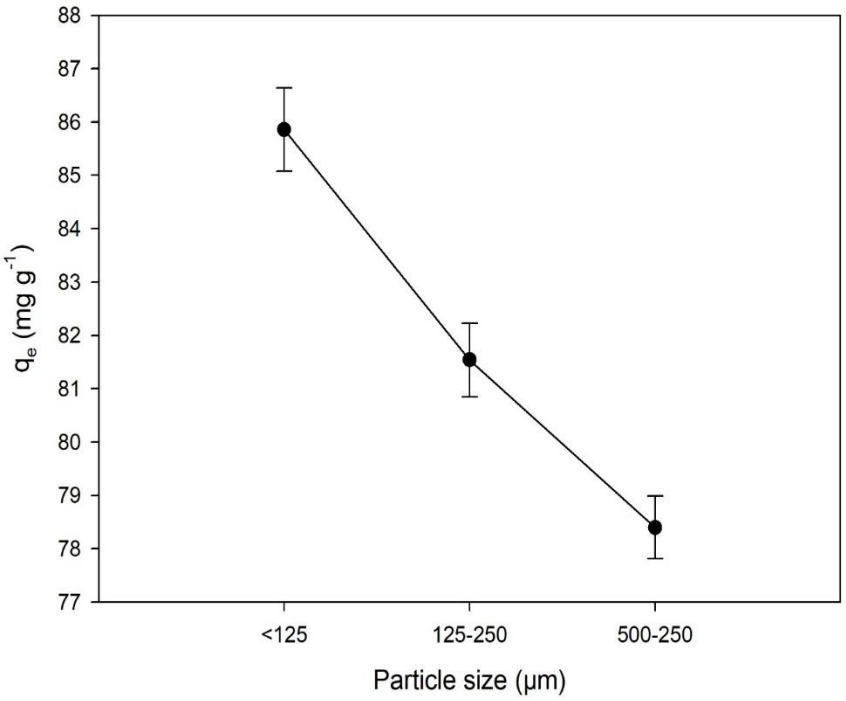

Figure 4.10 Effect of particle size of MO mix on the sorption of RR 120.

4.2.4 Effect of Adsorbent Dose

In the adsorption experiments, the interaction of MO seed mixture with four adsorbent amounts (0.5, 1, 2 and 4 g / L) and 50 mg / L RR 120 dye was carried out at pH 1. The effects of the adsorbent doses on the RR 120 adsorption are given in Figure 4.11. The amount of dye retained per gram of adsorbent is increased from 10.76 mg /g to 85.36 mg /g by MO when the adsorbent concentration is decreased to 0.5 g /L. The highest adsorption level was obtained in the 0.5 g / L adsorbent value ($p < 0.01$). It can limit the adsorption capacity due to the superposition of the adsorbent at high biomass concentration. Along with over accumulation of adsorbent, the adsorbent dye molecules cause less interaction and decrease the amount of adsorption. The removals of Reactive Red 194 and Direct Blue 53 on Kupuassu shell also increased by decreasing the adsorbent concentration (Cardoso et

al., 2011). Similar results have been observed in the treatment of Lanaset Red G with lentil straw (Çelekli et al., 2012). For this reason, 0.5 g / L of adsorbent dose was used in subsequent studies.

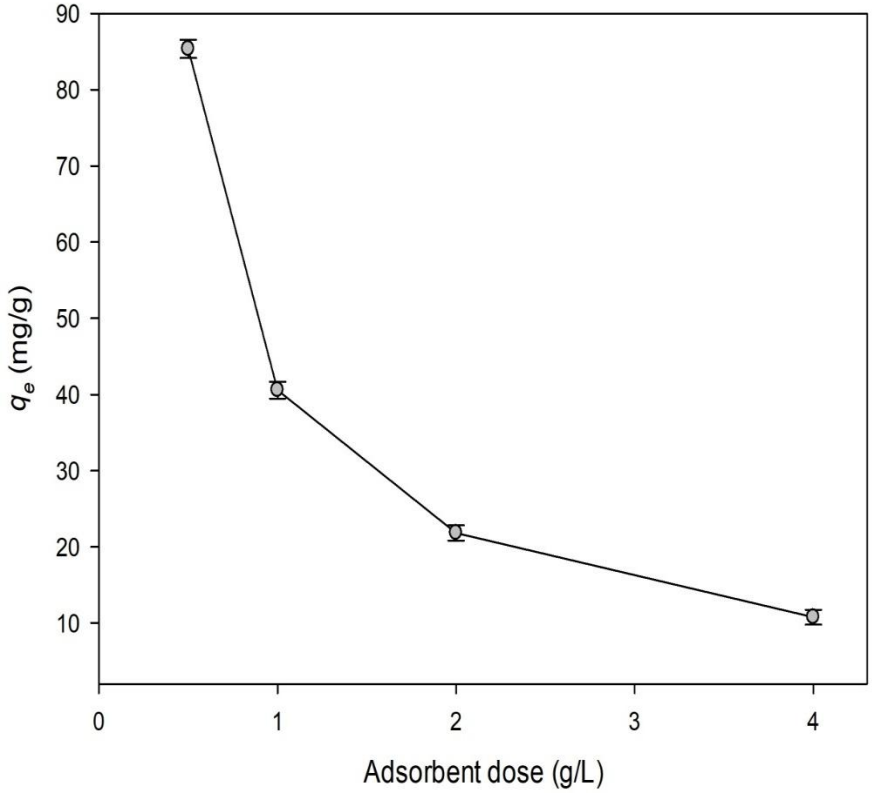

Figure 4.11 Effect of adsorbent dose on the adsorption of RR 120.

4.2.5 The Effect of Temperature

The temperature is one of the important parameters affecting the adsorption capacity and the adsorption process. MO seed mixture and adsorption of RR 120 were carried out at different temperature values (293, 303, 313 and 323 K). The effects of the temperature on the sorption process are shown in Figure 4.12. The results of the study showed that the sorption level of RR 120 decreased with increasing the ambient temperature of sorption solution. However there was no statistically significant difference in MO adsorption capacity among different temperature levels. This suggests that this process is mainly an exothermic interaction. The interaction between the adsorbent surface groups and the RR 120 molecules has been shown to decrease as the temperature increases.

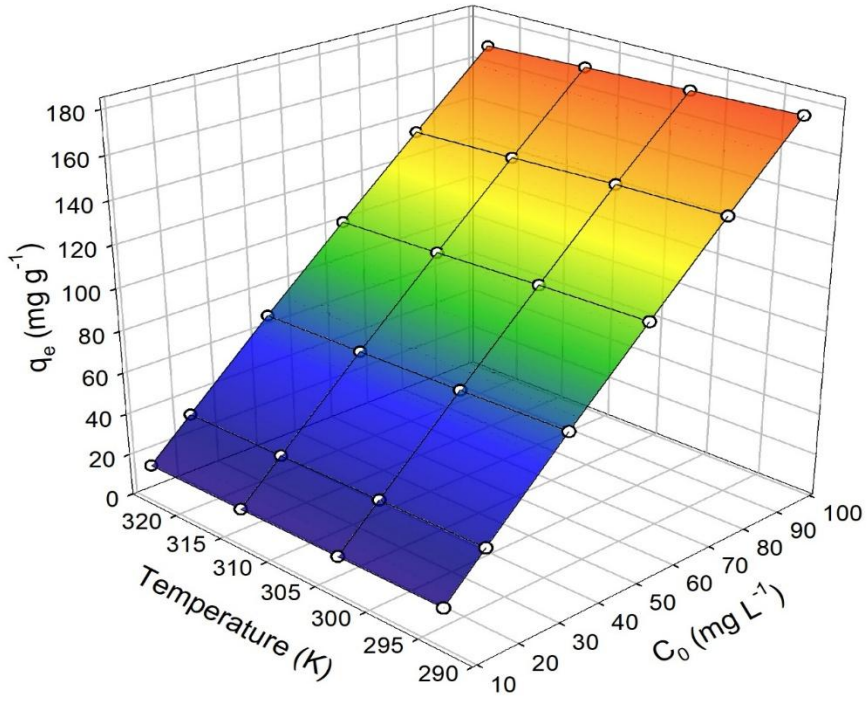

Figure 4.12 Effect of temperature on RR 120 sorption (<125 µm adsorbent particle size, pH 1 and m= 0.5 g / L).

4.2.6 Effects of Initial Dye Concentration and Interaction Time

The reactive dye adsorption capacity of the MO seed mixture was determined at initial of 10, 20, 40, 60, 80 and 100 mg / L RR 120 concentrations and t = 0-90 min of contact time at pH1. Effects of initial RR 120 concentration and interaction time on dye sorption (qt, mg / g) per unit adsorbent mass are shown in Figure 4.13.

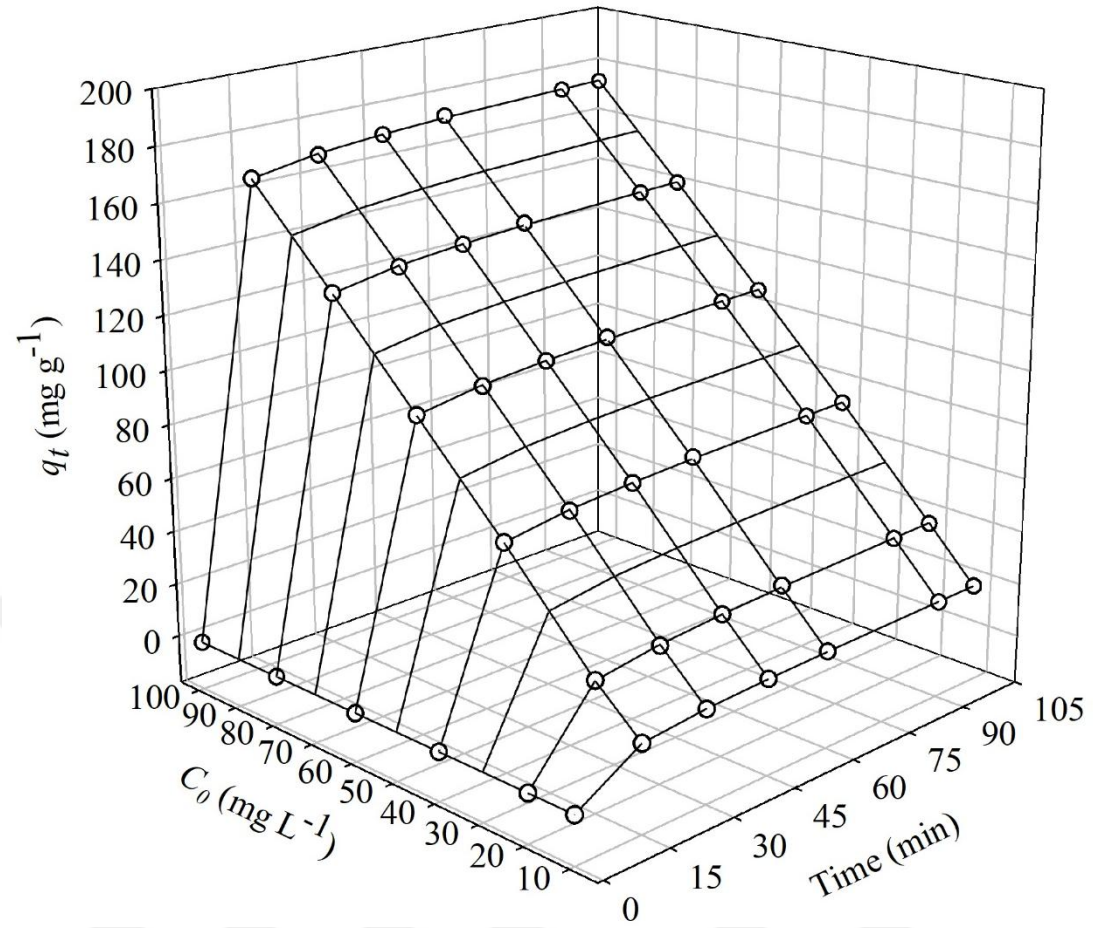

Figure 4.13 Effect of initial RR 120 concentration and contact time on the sorption capacity.

A statistically significant difference ($p < 0.01$) was observed in the amount of RR 120 retained by the MO seed mix as a result of raising the initial dye concentration from 10 mg / L to 100 mg / L. The maximum dye adsorption was obtained as 173.99 mg / g at 100 mg / L. The increase in the initial dye concentration provides an important impetus for the transfer of dye molecules between the aqueous phase and the solid phase (Doğan et al., 2009, Çelekli et al., 2010b). It is stated that the increase of the initial concentration has an important influence on the diffusion mechanism (Khataee et al., 2010; Wang et al., 2010). Reactive Red 120 with pistachio peel shell (Çelekli et al., 2010b), bentonite (Tabak et al., 2010), *Hydrilla verticillata* (Naveen et al., 2011) and *Chara contraria* (Çelekli et al., 2012 b).

The RR 120 was quickly removed from the aqueous sorption solution by the MO seed mix in the first 10 min of the run (Figure 3.13). Then the dye removal rate gradually decreasesed and continueds until the achievement of static equilibrium. (ARICA and Bayramoğlu, 2007; Çelekli et al., 2010; Tabak et al., 2010; Naveen et al., 2011; Çelekli et al., 2012b), as compared to other adsorbents.

4.3 Sorption kinetics

Conduct of sorption kinetic grants information to clarify sorption average and operative agents simulating the average, Pseudo second-order, logistic, Avrami and Elovich kinetic were conducted for the kinetic data. Pseudo-second-order kinetic model (Ho and Mckay 1995) it is one of the utmost applied kinetic models to characterize kinetic adsorption datum. Such kinetic model was utilized while appeared as:

$$\frac{t}{q_t} = \frac{1}{k * q_e^2} + \frac{t}{q_e}$$

Where, q_e and q_t display the dye sorbed on the sorbent (mg-/ g) at equilibrium while on time t (min), respectively. K is the pseudo-second-order average constant and the result of pseudo second-order was found in Fig (4.14).

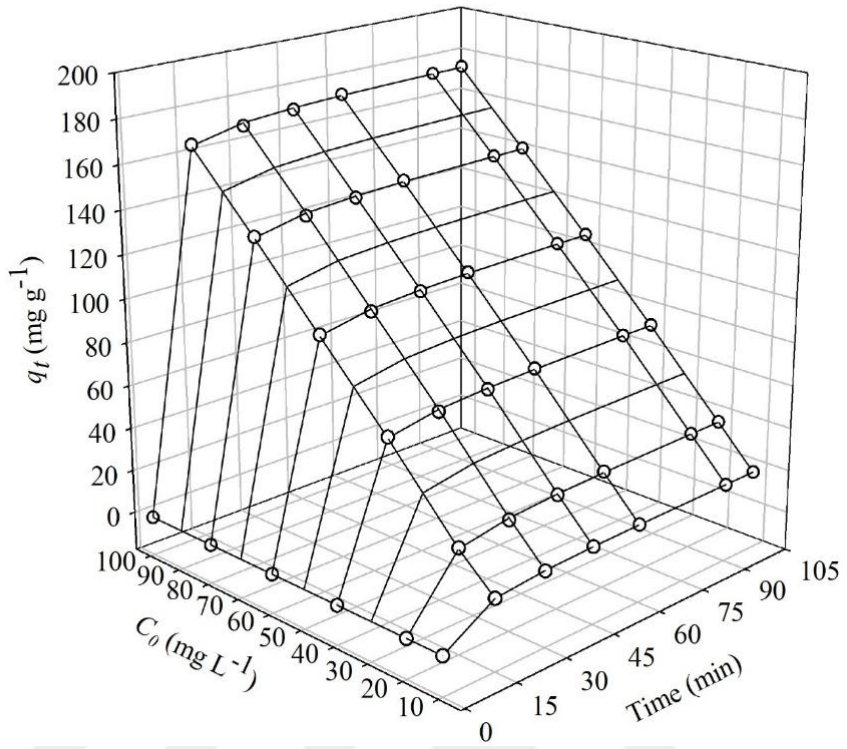

Figure 4.14 Nonlinear Pseudo second-order kinetic model for the sorption of RR 120 on MO seed Mix ((pH=1, particle size < 125 µm, m = 0.5 g/L, t = 100 min, and 293 K). Comparison between experimental points (circle) and fitted curves by the model with mesh lines.

Logistic model has been used into portend biomass, development of biovolume values via microorganisms (Çelekli et al., 2009). Newly, the logistic model has been suggested (Çelekli et al., 2010) to pick further input and characterize whole the sorption procedure. That model was adjusted into the experiential kinetic datum while expressed as

$$q_t = \frac{A}{1 + (\frac{t}{b})^c}$$

Where A is ceiling adsorption (asymptote value) in equilibrium, t is time (min) while qt is the amount from sorbed RR120 at MO (at milligrams per gram). Logistic constants are *b* and *a*. Logistic model was adjusted into experiential datum, not only into characterize the sorption from RR120 at MO but also into detect further input

about the adsorption kinetics like the ceiling dye uptake in equilibrium (A, at milligrams per gram), the lag time from adsorption (l, at minutes), while the adsorption average (μ, in per minute). The result of Logistic model was presented in Fig (4.15).

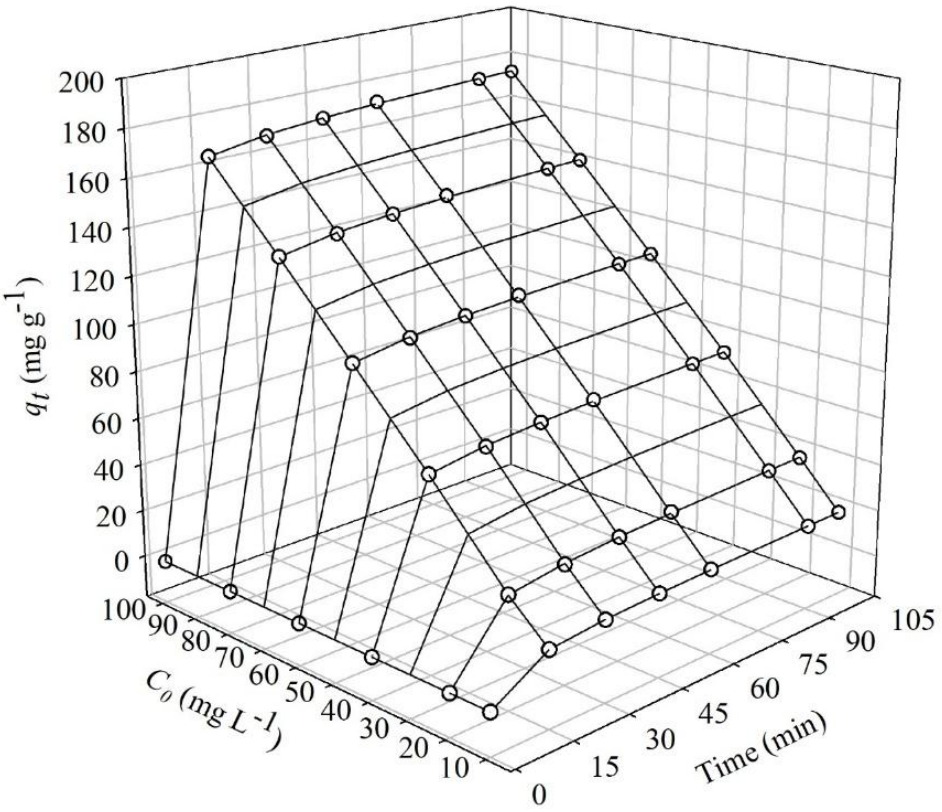

Figure 4.15 Logistic model for the sorption of RR 120 on MO mix ((ph=1, particle size < 125 μm, m = 0.5 g/l, t = 100 min, and 293 k). comparison between experimental points (circle) and fitted curves by the model with mesh lines.

Avrami kinetic model (Avrami 1939) was utilized to characterizing desorption while sorption kinetics of RR120 on the MO. That equation locates several kinetic parameters, like the possible variation from the sorption rates in the mission of the first concentricity while the sorption time. This equation was represented as

$$q_t = q_{epred} \{1 - \exp[-(K_{av} t)]^{n_{av}}$$

Wherever t is contact time, k_{av} is the regulated kinetic constant (at per minute) while nav is related to the sorption mechanism amidst the sorbent while sorbate (at minutes). The result of Avrami model was presented in Fig. 4.16.

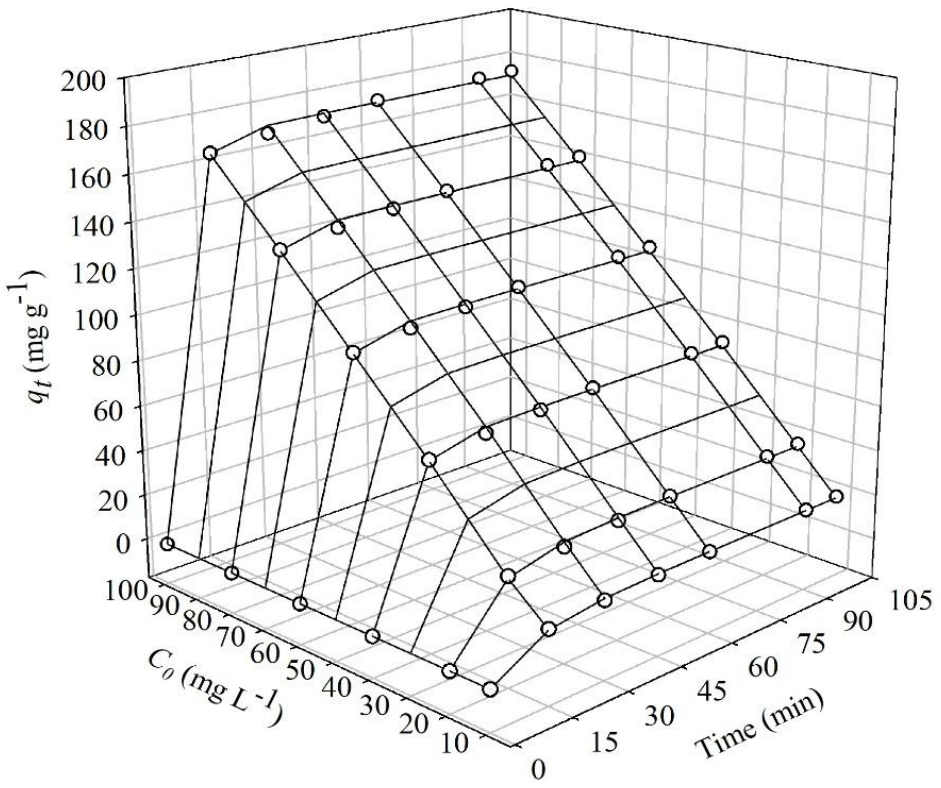

Figure 4.16 Nonlinear Avrami kinetic model for the sorption of RR 120 on MO seed mix ((ph=1, particle size < 125 µm, m = 0.5 g/l, t = 100 min, and 293 k). Comparison between experimental points (circle) and fitted curves by the model with mesh lines.

Elovich model (ÇELEKLI et al., 2013) is regarding existing tough surface that is energetically various while neither sorption nor could interactions amidst the sorbed types basically impact kinetics of sorption at minimum surface covering (ÇELEKLI et al., 2013). Such kinetic model was utilized while represented as

$$qt = \frac{1}{\beta} \ln\ (1 + \alpha\beta t)$$

Wherever α is the first sorption average while β is the sorption constant regarding the range from the exterior face covering while activation energy to chemisorption. Together, β and α, are the Elovich constants. The result of Elovich model was presented in Fig.4.17.

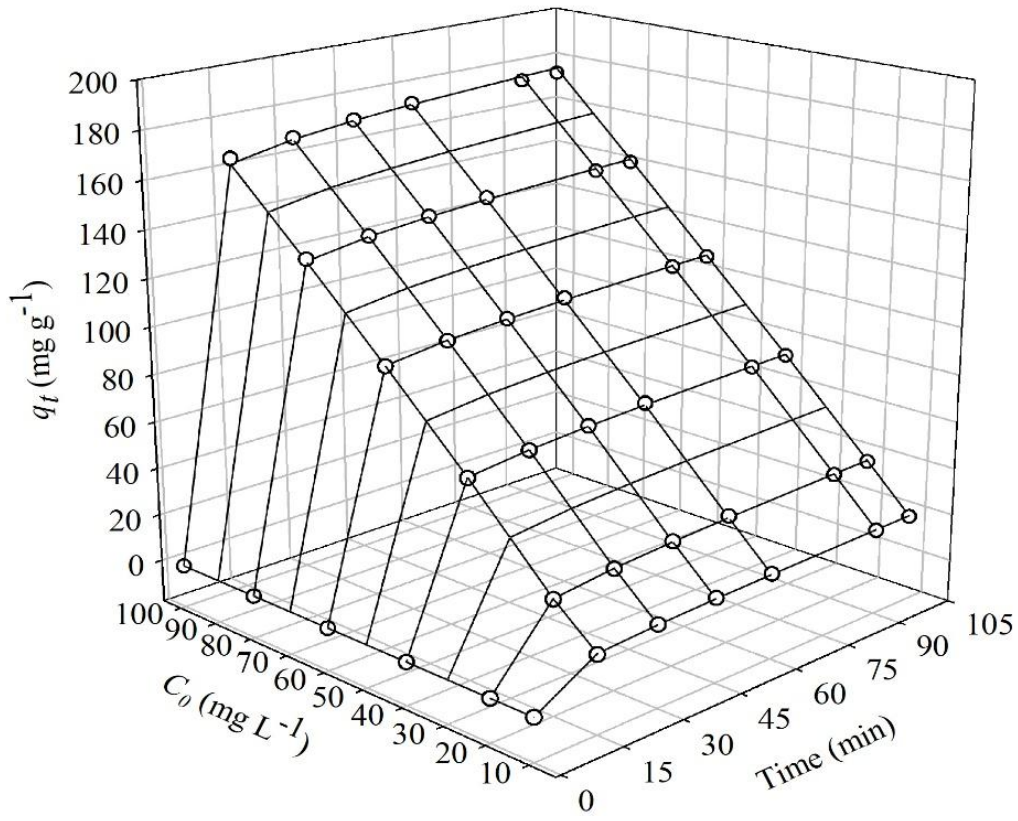

Figure 4.17 Nonlinear Elovich kinetic model for the sorption of RR 120 on the MO mix ((ph=1, particle size < 125 µm, m = 0.5 g/l, t = 100 min, and 293 k). Comparison between experimental points (circle) and fitted curves by the model with mesh lines.

Prophesy kinetic parameter while experiential datum (q_{exp}) are presented in Tables (4.4, 4.5, 4.6 and 4.7). Each kinetic models were perfectly adjusted to the experiential datum. The parameters of the pseudo second-order kinetics and logistic models are given in Table 4.4 and 4.5, respectively, at pH 1 at four temperatures and six initial RR 120 dye concentrations. The k-value of the pseudo second-order kinetic model constant ranged from 0.1706 to 1.0184 mg/g/min. The values of the model constant indicate that the MO and RR 120 are rapidly dispersed. This constant value increased as the ambient temperature decreased. The amount of paint retained on MO

by this model was found to be 17.85 to 173.52 mg/g (q_{pred}). There was no significant difference between the predicted values of the model and the experimental data ($p > 0.05$). The maximum adsorption level and adsorption ratio values as a result of the logistic model are shown in Table 4.5. The maximum adsorption of RR 120 with MO varied from 19.11 to 185.74 mg / g at 293 K, when initial RR120 increased from 10 mg/L to 100 mg/L. There was a correspondence between model data and experimental measured values ($p > 0.05$). The logistic model constant is between 0.91 and 11.00 mg/g/min. The sorption average (μ, mg/m/min) raised with lowering solution temperature. The reaction showed exothermic and high dye concentration was effective on dye diffusion.

Table 4.4 Pseudo-Second-Order Kinetic parameters for the sorption of RR120 on MO seed mix (pH1, m = 0.5 gL^{-1} , and t = 0-100 min).

K	C_0	q_{exp}	q_{pred}	K	R^2	RSS	SEE
293	10	18.55	18.50	0.1791	0.9998	0.0606	0.1005
	20	36.75	36.57	0.2006	0.9988	1.2944	0.4644
	40	72.70	72.38	0.4537	0.9996	1.6944	0.5314
	60	107.10	106.74	0.6448	0.9998	2.2700	0.6151
	80	141.00	140.62	0.8380	0.9998	2.6121	0.6598
	100	173.99	173.52	1.0184	0.9999	3.1441	0.7239
303	10	18.30	18.25	0.1759	0.9998	0.0597	0.0998
	20	36.16	36.01	0.1971	0.9987	1.0268	0.4597
	40	71.63	71.29	0.4450	0.9996	1.7034	0.5329
	60	106.21	105.85	0.6385	0.9998	2.2712	0.6152
	80	140.02	139.63	0.8308	0.9998	2.6219	0.6611
	100	171.95	171.51	1.0083	0.9999	3.0954	0.7183
313	10	18.10	18.05	0.1732	0.9998	0.0591	0.0993
	20	35.80	35.63	0.1963	0.9987	1.2700	0.4601
	40	70.80	70.48	0.4399	0.9996	1.6806	0.5293
	60	104.70	104.34	0.6286	0.9997	2.2597	0.6137
	80	137.90	137.52	0.8179	0.9998	2.6035	0.6587
	100	170.10	169.63	0.9939	0.9999	3.1361	0.7230
323	10	17.90	17.85	0.1706	0.9996	0.0549	5.3004
	20	35.50	35.33	0.1914	0.9984	1.0763	6.0179

	40	70.20	69.88	0.4356	0.9995	1.6369	4.8291
	60	103.50	130.11	0.6206	0.9997	2.2534	0.6448
	80	136.20	135.82	0.8069	0.9998	2.6129	5.1423
	100	168.20	167.73	0.9819	0.9999	3.1561	11.6225

Table 4.5 Logistic Kinetic parameters for the sorption of RR120 on MO seed mix (pH1, m = 0.5 gL $^{-1}$, and t = 0-100 min).

K	C_0	q_{exp}	A	μ	R^2	RSS	SEE
293	10	18.55	19.74	0.95	0.9998	0.0554	0.0954
	20	36.75	42.94	1.95	0.9988	0.0623	0.3223
	40	72.70	80.36	4.33	0.9996	0.5904	0.3137
	60	107.10	116.00	6.58	0.9998	0.8010	0.3674
	80	141.00	150.62	8.82	0.9998	0.9339	0.3945
	100	173.99	185.74	11.00	0.9999	1.0543	0.4191
303	10	18.30	19.53	0.93	0.9998	0.0544	0.0952
	20	36.16	42.14	1.91	0.9987	0.6367	0.3258
	40	71.63	79.42	4.26	0.9996	0.5812	0.3115
	60	106.21	115.13	6.52	0.9998	0.8071	0.3668
	80	140.02	149.74	8.76	0.9998	0.9266	0.3920
	100	171.95	183.21	10.87	0.9999	1.0744	0.4231
313	10	18.10	19.32	0.92	0.9998	0.0543	0.0951
	20	35.80	41.91	1.88	0.9987	0.6217	0.3219
	40	70.80	78.41	4.20	0.9996	0.5899	0.3136
	60	104.70	113.56	6.42	0.9997	0.8096	0.3673
	80	137.90	147.49	8.62	0.9998	1.0535	0.3944
	100	170.10	181.81	10.05	0.9999	1.0535	0.4190
323	10	17.90	19.11	0.91	0.9996	0.0541	0.0950
	20	35.50	41.58	1.86	0.9984	0.6212	0.3218
	40	70.20	77.79	4.16	0.9995	0.5898	0.3135
	60	103.50	112.34	6.34	0.9997	0.8094	0.3673
	80	136.20	145.77	8.50	0.9998	0.9336	0.3944
	100	168.20	179.89	10.62	0.9999	1.0534	0.4190

Correlation coefficient and error analysis values were used to compare the kinetic model performances used in the study. The correlation coefficient (R2) of the pseudo second order kinetic model varied from 0.9984 to 0.9999. On the other hand, according to the Logistic model, R^2 value was calculated as 0.9994 to 0.9999. According to the sum of squares of errors (SSE) analysis, pseudo second order is found between 0.0993 – 11.6225 and Logistic model is between 0.0950 – 0.4231. Results of the smaller error analysis and higher R^2 indicated that the logistic model RR 120 is better suited to explain the adsorption on MO. The values calculated from the logistic model were in good agreement with the experimental data (Figure 4.15). The pseudo second-order kinetic model also well fitted and showed very few deviations at high RR 120 concentrations.

The parameters of the Avrami and Elovich models are given in Table 4.6 and 4.7, respectively. The k-value of the avrami kinetic model constant ranged from 0.976 to 1.452 and nav related to the adsorption mechanism ranged from 0.0976 to 0.1452. Both of them increases with temperature decreases.

The β-value of the elovich kinetic model constant ranged from 0.144 to 0.454 increases with temperature increases

Table 4.6 Avrami Kinetic parameters for the sorption of RR120 on MO seed mix (pH1, m = 0.5 gL $^{-1}$, and t = 0-100 min).

K	C_0	n_{av}	k_{av}	A	R^2	RSS	SEE
293	10	0.0991	0.989	18.0284	0.9951	1.2878	0.463
	20	0.1028	1.028	35.636	0.9919	8.4718	1.188
	40	0.1254	1.258	71.2192	0.9971	12.2080	1.426
	60	0.1343	1.342	105.4408	0.9983	15.6240	1.613
	80	0.1406	1.405	139.2436	0.9990	17.6240	1.713
	100	0.1452	1.452	172.0801	0.9992	19.8880	1.820
303	10	0.0985	0.984	17.7871	0.9951	1.2626	0.458
	20	0.1023	1.022	35.0864	0.9918	8.2718	1.174
	40	0.1249	1.248	70.1296	0.9970	12.2328	1.427
	60	0.1341	1.340	104.5441	0.9983	15.6251	1.613
	80	0.1404	1.403	138.2483	0.9989	17.6643	1.715
	100	0.1451	1.449	170.0769	0.9992	19.675	1.810
313	10	0.0981	0.984	17.5917	0.9951	1.2419	0.454
	20	0.1018	1.017	34.7054	0.9916	8.2709	1.174
	40	0.1246	1.245	69.3269	0.9970	12.1112	1.420
	60	0.1337	1.336	103.0456	0.9983	15.5527	1.610
	80	0.1402	1.400	136.1472	0.9989	17.5687	1.711
	100	0.1447	1.446	168.1888	0.9992	19.8386	1.818
323	10	0.0976	0.976	17.3964	0.9950	1.2208	0.451
	20	0.1014	1.014	34.412	0.9915	8.2053	1.162
	40	0.1243	1.241	68.7295	0.9969	12.079	1.418
	60	0.1333	1.333	101.8481	0.9982	15.5169	1.608
	80	0.1397	1.397	134.4493	0.9989	17.5368	1.709
	100	0.1444	1.444	166.2904	0.9992	19.8135	1.817

Table 4.7 Elovich Kinetic parameters for the sorption of RR120 on MO seed mix (pH1, m = 0.5 gL $^{-1}$, and t = 0-100 min).

K	C_0	β	R^2	RSS	SEE
293	10	0.454	0.9981	0.4974	0.287
	20	0.246	0.9990	1.0161	0.411
	40	0.240	0.9998	1.0090	0.410
	60	0.218	0.9999	1.3110	0.467
	80	0.177	0.9999	3.8979	0.805
	100	0.144	0.9995	12.9900	1.471
303	10	0.454	0.9981	0.4975	0.287
	20	0.247	0.9986	1.0500	0.418
	40	0.241	0.9998	0.9869	0.405
	60	0.219	0.9999	1.2986	0.465
	80	0.178	0.9998	3.6742	0.782
	100	0.145	0.9995	12.3390	1.434
313	10	0.454	0.9980	0.4976	0.287
	20	0.246	0.9990	1.0159	0.411
	40	0.240	0.9997	1.0087	0.410
	60	0.221	0.9998	1.2984	0.465
	80	0.180	0.9998	3.3526	0.747
	100	0.147	0.9995	11.1365	1.376
323	10	0.454	0.9980	0.4977	0.287
	20	0.246	0.9990	1.0160	0.411
	40	0.240	0.9997	1.0087	0.410
	60	0.222	0.9998	1.2982	0.465
	80	0.182	0.9998	3.9550	0.717
	100	0.148	0.9995	10.6132	1.329

The correlation coefficient (R^2) of Avrami kinetic model was varied from 0.9915 to 0.9992. On the other hand, according to the Elovich model, R^2 value was calculated as 0.9980 to 0.9999. According to the sum of squares of errors (SSE) analysis,

Avrami is found between 1.162 – 1.820 and Alovich model is between 0.287 – 1.471.

4.4 Sorption Isotherm

At several dye concentration while in four temperature (293–323 K) under optimum operating status equilibrium modeling were executed (pH 1, a particle size of ≤125 μm, and sorbent dose of 0.5 g/L). Tempkin, Dubinin Radushkevish, Freundlich and Langmuir isotherms were utilized in the existent study.

Langmuir isotherm (Langmuir, 1918), investigated as a monolayer adsorption while expressed as:

$$\frac{C_e}{q_e} = \frac{1}{q_L * K_L} + \frac{C_e}{q_L}$$

$$R_L = \frac{1}{1 + (K_L * C_o)}$$

Wherever *b* is the Langmuir constant related to energy from the adsorption, q_L is the monolayer adsorption capability, *Ce* is the equilibrium dye concentricity in solution and *qe* is the equilibrium dye concentricity on the sorbent.

Multilayer adsorption is deduced by simulating a different adsorption exterior face with interaction amidst adsorbed molecules and Freundlich isotherm (Freundlich 1906) appeared:

$$\log q_e = \log K_f + \frac{1}{n} * \log C_e$$

Wherever Freundlich constants, *n* and K_f, adsorption density and the sorption ability of adsorbent, respectively.

Temkin isotherm (Temkin 1940) takes to account from sorbent–sorbate interaction while supposes this liberate energy from adsorption is a function from the exterior face covering.

$$qe = \frac{RT}{bt} \ln At + \left(\frac{RT}{bt}\right) \ln Ce$$

At that isotherm, at is the equilibrium bound constant identical into the extreme bound energy while constant bt is linked to heat from adsorption. Worth's from above-mentioned constants (Table 4.9) decrease when temperature increased from 293 *K* to 323 *K*, specified that adsorption from RR 120 on MO is exothermic. That isotherm was quite fitted to equilibrium datum, submitted that this sorption is described via a regular division from bound ability up into ultimate bound energy.

Dubinin–Radushkevish (D–R) isotherm (Dubinin and Radushkevich 1947) suppose this there is multilayer character from adsorption possibility wherever liberate energy from adsorption is attached to grade from pore filling. D–R isotherm is qualified as:

$$\ln q_e = \ln q_m - \beta\varepsilon^2$$

$$\varepsilon = R * T * \ln\left(1 + \frac{1}{C_e}\right)$$

Where q_m is the maximum adsorption ability (mg g^{-1}), *T* is temperature (*K*), *R* is the gas constant (8.314 $Jmol^{-1}$ K^{-1}), ε is the Polanyi potential, and *β* is a constant attached to the sorption energy (mol*2* kJ-*2*).

From adsorption per molecule from sorbate when it is transported into the solid of infinity at the resolution, Values from β give the mean free energy, E (kJ mol^{-1}). Results from equilibrium models are presented in Table (4.9). The temperature was an increase of 293 *K* to 323 *K*, Monolayer sorption ability decrease from 412.32 to 172.43 mg g^{-1}. This specified this the adsorption procedure is an exothermic reaction.

Freundlich while Langmuir isotherms have height attachment stage to characterize the adsorption of RR 120 on the MO (Table 4.9). However, Freundlich model had higher correlation coefficient values (R^2=0.9974–0.9981) than those of Langmuir model (R^2=0.9841–0.9896).

Table 4.8 The values of isotherm parameters for the removal of RR120 on MO seed (pH1, particle size < 125 μm , Co = 10-100 mgL $^{-1}$, m = 0.5 gL $^{-1}$, and t = 0-100 min).

İsotherm	Parameter	293 K	303 K	313 K	323 K
Freundlich	K_f	12.488	10.7416	9.7084	8.9447
	n_f	1.2922	1.2346	1.2232	1.2132
	R^2	0.9974	0.9981	0.9986	0.9981
	RSS	0.0018	0.0013	0.0009	0.0013
	SEE	0.0032	0.0026	0.0029	0.0026
Langmuir	b_0	0.0744	0.054	0.0465	0.0419
	ql	172.43	198.38	204.06	206.66
	R^2	0.9841	0.9878	0.9855	0.9896
	RSS	0.00006	0.00004	0.00005	0.00004
	SEE	0.0173	0.0149	0.0127	0.0149
Dubinin-Raduskevish	*Qm*	57.61	56.55	55.71	55.42
	β	-0.4348	-0.5041	-0.5518	-0.6012
	R^2	0.8309	0.8176	0.8161	0.8230
	RSS	0.6216	0.6744	0.6784	0.6519
	SEE	0.3219	0.3353	0.3362	0.3296
Temkin	*A*	1.4613	1.2168	1.0905	0.9971
	β	- 1.0181	-0.986	-0.99	- 0.9915
	R^2	0.9434	0.9398	0.9375	0.9403
	RSS	257	268	272	253
	SEE	6.544	6.693	6.733	6.499

Sorption abilities from reactive dyes on diverse adsorbents parallel with offered in Table (4.10). MO given favorable adsorption ability to the abstraction of reactive dye parallel to *Jatropha curcas* shells (Prola et al., 2013), Indian *Jujuba* seeds (Reddy et al., 2012), and *Eucalyptus* wood sawdust (Mane et al., 2013). The adsorption ability from MO was decrease than these of *H. verticillata* (Naveen et al., 2011) and pistachio husk (Çelekli et al., 2010) into the sorption of RR 120. The divergence in ultimate adsorption competence from different sorbents power be due to variation in kind while amount from practical groups at their frameworks while adsorption mechanisms of different sorbents while experiential status.

Table 4.9 Sorption abilities of reactive dyes on several sorbents

Adsorbent	Adsorbate	q_{max}	References
Pumpkin husk	Lanaset Red G	436.28	Çelekli et al., 2013
Cashew nut shell	Congo Red	5.18	Kumar et al., 2010
Used tea leaves	Acid Blue15	126.53	Adegoke et al., 2015
Bengal gram seed husk	Congo Red	41.66	Reddy et al., 2013
Rice husk ash	Indigo carmine	65.90	Lakshmi et al., 2009
***Eucalyptus* wood saw dust**	Congo Red	66.67	Mane et al., 2013
***Jujuba* seed**	Congo Red	55.56	Reddy et al., 2012
Mangrove bark	Direct red-23	21.55	Tan et al., 2010
***Jatropha curcas* shells**	RR 120	65.63	Prola et al., 2013
Chara contraria	RR 120	112.83	Çelekli et al., 2012
Teak tree bark	Methylene blue	333.3	Adegoke et al., 2015
Hydrilla verticillata	RR 120	120.85	Naveen et al., 2011
Pistachio husk	RR 120	324.88	Çelekli et al., 2010
Tapioca peel	Red brown C4R	121.47	Parvathi, et al., 2010
***Moringa oleifera* seeds**	RR120	412.32	This study

Mean free energy [E (kJ mol^{-1})] could be utilized into recognizing chemical and physical adsorption of dyes molecules. That energy could be fated from D R model, utilize the following relation:

$$E = \frac{1}{\sqrt{2\beta}} \quad (4.1)$$

Where β is a constant linked to adsorption energy. Value of E is lower than 8 kJ mol^{-1} describe physical sorption, whilst its medium free energy varied between 8 and 16 kJ mol^{-1} describe chemical sorption (Chen et al., 2011). At the existent study, the value from E was set up into being lower than 8 kJ mol^{-1}, who specified adsorption from RR 120 at the MO was physical.

4.5 Activation Parameters

Arrhenius equation (Anirudhan and Radhakrishnan 2008) was applied to locate activation energy (E_a) to the adsorption from RR 120 on MO. Pseudo-second average constant (k) was not only applied, but too adsorption average (μ) of logistic model was utilized to Arrhenius equation into figure activation energy. That equation is expressed as:

$$\ln K = \ln A - \frac{E_a}{RT} \quad (4.2)$$

Where T is the ultimate temperature (K), R is the gas constant (8.314 J mol−1 K^{-1}), Ea is the activation energy (kJ mol^{-1}) and A is the Arrhenius constant. Size from Ea grants input, on sorption kind all chemical or physical. Whether sorption procedure requests lower energy in extent of 5 to 40 kj mol^{-1}, who is volatile while physical. Reciprocally, powerful forces while high activation energy is wanted (between 40 while 800 kj mol^{-1}) to alchemical adsorption. Ea to the adsorption from RR 120 by MO was set up as 0.86 and 1.39 kj mol^{-1} by utilizing of logistic sorption rate and pseudo second constant, respectively. Values of E_a specified this the adsorption of reactive red 120 on MO was an exothermic and physical character.

4.6 Thermodynamic Parameters

Into estimate while pick input about the adsorption procedure like impulsive or not while endothermic or exothermic, thermodynamic parameters (standard free energy changes ΔG°, kJ mol^{-1}), entropy changes (ΔS°, J mol-1 K^{-1}), while enthalpy changes (ΔH°, kJ mol^{-1})] were utilized in the next equations:

$$\Delta G° = RTln\,(KL)$$

$$\Delta G° = \Delta H° - T\Delta S°$$

Where T is temperature (K), K_L is Langmuir constant (l mol^{-1}) and R is the global gas constant (8.314 J mol^{-1} K). Values of ΔS° and ΔH° can be determined of the slope and object of a plot of ln KL versus 1/T.

Table 4.10 Thermodynamic parameters for the adsorption of RR120 on MO seed (pH1, particle size < 125 μm , Co = 10-100 mgL^{-1} , m = 0.5 gL^{-1} , and t = 0-100 min).

T (K)	***ΔG° (kJ mol^{-1})***	***ΔH° (kJ mol^{-1})***	***ΔS° (kJ mol^{-1} K^{-1})***
298	-28.26	-14.635	-0.046
308	-28.42		
318	-28.97		
328	-29.62		

Outcomes are presented in Table (4.11). A negative value of ΔH° specified that the adsorption procedure was exothermic. The difference in free energy amidst −20 and 0 kJ mol^{-1} specified physical adsorption, while the energy extends from −80 to −400kJ mol^{-1} display chemical adsorption. Values from ΔG° varying from -28.26 to -29.62 kJ mol^{-1} specified this adsorption was mainly physical. Besides, the negative value from ΔG° specified that procedure is existence practical and impulsive nature of adsorption.(Çelekli et al., 2014).

CHAPTER V
CONCLUSION

In this research, *Moringa oleifera* (MO) seeds were used as an eco-friendly material in the process of purification of water contaminated with dye RR120 as a laboratory solution to know the effect of *Moringa* seeds on it and for several reasons mentioned earlier, including low cost and availability and the absence of any side effects when used in laboratory experiments.

The effects of initial pH, adsorbent dose, particle size, initial RR 120 values, contact time and temperature on the adsorption capacity were studied by using of (MO) mix. Mathematical data were used to describe kinetic, isotherm and thermal data. The results of this study were summarized as follows:

SEM analysis, in the natural appearance of the dried MO shell, no breakage was observed and numerous pores were seen. After the RR 120 removal, it is thought that the pores in the surface of the adsorbent have been shrunk so that they can play an important role in increasing the adsorption capacity.

FTIR-ATR analysis indicate that, amino acid, carbonyl, and amide groups on the MO seed mixture played significant roles on the sorption of RR 120.

The pH_{zpc} of (MO) mix was found to be 4.5. Lower pH values than pH_{zpc} favorite the adsorption of anionic dye such as RR 120 due to the electrostatic attraction with becoming positively charged of adsorbent exterior face. The extreme adsorption was measured at pH1.

The adsorption ability of MO increased when the particle size was reduced to <125 µm at 250-500 µm.

Adsorption ability significantly increase with decrease the adsorbent dose.

In Effect of MO type, the maximum adsorption of RR120 was found on (MO) mix. MO mix had great capacity for the adsorption of RR 120 Because of the increased absorption area of the absorbed molecules in solution.

The results of the study showed that the adsorption level of RR 120 decreased with the ambient temperature increased MO seed mixture. This suggests that this process is an exothermic interaction.

The maximum dye adsorption was obtained at an initial dye concentration.

The k-value of the pseudo second-order kinetic model constant ranged from 0.1706 to 1.0184 mg / g / min. The values of the model constant indicate that the MO and RR 120 are rapidly dispersed. This constant value increased as the ambient temperature decreased. The amount of dye retained on MO by this model was found to be 17.85 to 173.52 mg / g (q_{pred}). There was no significant difference between the predicted values of the model and the experimental data ($p > 0.05$).

The maximum adsorption level and adsorption ratio values as a result of the logistic model. The maximum adsorption of RR 120 with MO varied from 19.11 to 185.74 mg / g. There was a correspondence between model data and experimental measured values ($p > 0.05$). The logistic model constant is between 0.91 and 11.00 mg/g/min. The sorption average (μ, mg/g/min) raise to lowering temperature. As the temperature and dye concentration increased, the adsorption rate decreased. The reaction showed exothermic and high dye concentration was effective on dye diffusion.

From adsorption per molecule from adsorbate when it is transported into the solid of infinity at the resolution, Values from β give the mean free energy, E (kJ mol^{-1}). The temperature was an increase of 293 to 323 K, Monolayer sorption ability increase from 172.43 to 412.32 mg g-1. This specified this the adsorption procedure is an exothermic reaction.

Freundlich while Langmuir isotherms have height attachment stage to characterize the adsorption of RR 120 on MO Table.7. However, Freundlich model had higher correlation coefficient values (R^2=0.9974–0.9981) than these from Langmuir model (R^2=0.9841–0.9896).

E_a to the adsorption from RR 120 by MO was set up as 0.86 and 1.39 kj mol^{-1} by utilizing of logistic sorption rate and pseudo second constant, respectively. Values of E_a specified this the adsorption of reactive red 120 on MO was an exothermic and physical character.

A negative value of ΔH° specified that the adsorption procedure was exothermic. The difference in free energy amidst −20 and 0 kJ mol^{-1} specified physical adsorption, while the energy extends from −80 to −400 kJ mol^{-1} display alchemical adsorption. Values from ΔG° varying from -28.26 to -29.62 kJ mol^{-1} specified this adsorption was mainly physical. Besides, the negative value from ΔG° specified that procedure is existence practical and impulsive nature of adsorption.

REFERENCES

Mohan, N., Balasubramanian, N., Basha, C. A. (2007). Electrochemical oxidation of textile wastewater and its reuse. *Journal of hazardous materials*. **147(1-2)**, 644-651.

Sharma, M. K., Sobti, R. C. (2000). Rec effect of certain textile dyes in Bacillus subtilis. *Mutation Research/Genetic Toxicology and Environmental Mutagenesis*. **465(1)**, 27-38.

Malik, R., Ramteke, D. S., Wate, S. R. (2007). Adsorption of malachite green on groundnut shell waste based powdered activated carbon. *Waste management*. **27(9)**, 1129-1138.

Kadirvelu, K., Kavipriya, M., Karthika, C., Radhika, M., Vennilamani, N., Pattabhi, S. (2003). Utilization of various agricultural wastes for activated carbon preparation and application for the removal of dyes and metal ions from aqueous solutions. *Bioresource technology*. **87(1)**, 129-132.

Shen, D., Fan, J., Zhou, W., Gao, B., Yue, Q., Kang, Q. (2009). Adsorption kinetics and isotherm of anionic dyes onto organo-bentonite from single and multisolute systems. *Journal of hazardous materials*. **172(1)**, 99-107.

Chiou, M. S., Ho, P. Y., Li, H. Y. (2004). Adsorption of anionic dyes in acid solutions using chemically cross-linked chitosan beads. *Dyes and pigments*. **60(1)**, 69-84.

Lee, J. W., Choi, S. P., Thiruvenkatachari, R., Shim, W. G., Moon, H. (2006). Evaluation of the performance of adsorption and coagulation processes for the maximum removal of reactive dyes. *Dyes and pigments*. **69(3)**, 196-203.

Yagub, M. T., Sen, T. K., Afroze, S., Ang, H. M. (2014). Dye and its removal from aqueous solution by adsorption: a review. *Advances in colloid and interface science*. **209**, 172-184.

Rocha, J. H. B., Solano, A. M. S., Fernandes, N. S., da Silva, D. R., Peralta-Hernandez, J. M., Martínez-Huitle, C. A. (2012). Electrochemical degradation of remazol red BR and novacron blue CD dyes using diamond electrode. *Electrocatalysis*. **3(1)**, 1-12.

Dawood, S., Sen, T. K., Phan, C. (2014). Synthesis and characterisation of novel-activated carbon from waste biomass pine cone and its application in the removal of congo red dye from aqueous solution by adsorption. *Water, Air, & Soil Pollution*. **225(1)**, 1818.

Vijayaraghavan, K., Yun, Y. S. (2008). Biosorption of CI Reactive Black 5 from aqueous solution using acid-treated biomass of brown seaweed Laminaria sp. *Dyes and Pigments*. **76(3)**, 726-732.

Aksu, Z., Karabayır, G. (2008). Comparison of biosorption properties of different kinds of fungi for the removal of Gryfalan Black RL metal-complex dye. *Bioresource Technology*. **99(16)**, 7730-7741.

Paul, J., Rawat, K. P., Sarma, K. S. S., Sabharwal, S. (2011). Decoloration and degradation of Reactive Red-120 dye by electron beam irradiation in aqueous solution. *Applied Radiation and Isotopes*. **69(7)**, 982-987.

Royer, B., Cardoso, N. F., Lima, E. C., Vaghetti, J. C., Simon, N. M., Calvete, T., Veses, R. C. (2009). Applications of Brazilian pine-fruit shell in natural and carbonized forms as adsorbents to removal of methylene blue from aqueous solutions—Kinetic and equilibrium study. *Journal of Hazardous Materials*. **164(2-3)**, 1213-1222.

Royer, B., Cardoso, N. F., Lima, E. C., Macedo, T. R., Airoldi, C. (2010). A useful organofunctionalized layered silicate for textile dye removal. *Journal of hazardous materials*. **181(1-3)**, 366-374.

Carneiro, P. A., Umbuzeiro, G. A., Oliveira, D. P., Zanoni, M. V. B. (2010). Assessment of water contamination caused by a mutagenic textile effluent/dyehouse effluent bearing disperse dyes. *Journal of Hazardous Materials*. **174(1-3)**, 694-699.

Asouhidou, D. D., Triantafyllidis, K. S., Lazaridis, N. K., Matis, K. A., Kim, S. S., Pinnavaia, T. J. (2009). Sorption of reactive dyes from aqueous solutions by ordered hexagonal and disordered mesoporous carbons. *Microporous and Mesoporous Materials*. **117(1-2)**, 257-267.

Pearce, C. I., Lloyd, J. R., Guthrie, J. T. (2003). The removal of colour from textile wastewater using whole bacterial cells: a review. *Dyes and pigments*. **58(3)**, 179-196.

Lazaridis, N. K., Karapantsios, T. D., Georgantas, D. (2003). Kinetic analysis for the removal of a reactive dye from aqueous solution onto hydrotalcite by adsorption. *Water Research*. **37(12)**, 3023-3033.

Devi, R., Singh, V., Kumar, A. (2008). COD and BOD reduction from coffee processing wastewater using Avacado peel carbon. *Bioresource technology*. **99(6)**, 1853-1860.

Janoš, P., Šmídová, V. (2005). Effects of surfactants on the adsorptive removal of basic dyes from water using an organomineral sorbent—iron humate. *Journal of colloid and interface science*. **291(1)**, 19-27.

Zhu, L., Ma, J. (2008). Simultaneous removal of acid dye and cationic surfactant from water by bentonite in one-step process. *Chemical Engineering Journal*. **139(3)**, 503-509.

Sulak, M. T., Demirbas, E., Kobya, M. (2007). Removal of Astrazon Yellow 7GL from aqueous solutions by adsorption onto wheat bran. *Bioresource technology*. **98(13)**, 2590-2598.

Srivastava, V. C., Mall, I. D., Mishra, I. M. (2007). Adsorption thermodynamics and isosteric heat of adsorption of toxic metal ions onto bagasse fly ash (BFA) and rice husk ash (RHA). *Chemical Engineering Journal*. **132(1-3)**, 267-278.

Brillas, E., Martínez-Huitle, C. A. (2015). Decontamination of wastewaters containing synthetic organic dyes by electrochemical methods. An updated review. *Applied Catalysis B: Environmental*. **166**, 603-643.

Solís, M., Solís, A., Pérez, H. I., Manjarrez, N., Flores, M. (2012). Microbial decolouration of azo dyes: a review. *Process Biochemistry*. **47(12)**, 1723-1748.

Klavarioti, M., Mantzavinos, D., Kassinos, D. (2009). Removal of residual pharmaceuticals from aqueous systems by advanced oxidation processes. *Environment international*. **35(2)**, 402-417.

Falowo, A. B., Mukumbo, F. E., Idamokoro, E. M., Lorenzo, J. M., Afolayan, A., Muchenje, V. (2018). Multi-functional application of Moringa oleifera Lam. in nutrition and animal food products: A review. *Food Research International*.

Kumari, P., Sharma, P., Srivastava, S., Srivastava, M. M. (2005). Arsenic removal from the aqueous system using plant biomass: a bioremedial approach. *Journal of Industrial Microbiology and Biotechnology*. **32(11-12)**, 521-526.

Katayon, S., Ng, S. C., Johari, M. M., Ghani, L. A. (2006). Preservation of coagulation efficiency ofMoringa oleifera, a natural coagulant. *Biotechnology and bioprocess engineering*. **11(6)**, 489-495.

Oludoro, A. O., Aderiye, B. I. (2007). Efficacy of Moringa oleifera seed extract on the microflora of surface and underground water. *J Plant Sci*. **2**, 453-458.

Pritchard, M., Mkandawire, T., Edmondson, A., O'neill, J. G., Kululanga, G. (2009). Potential of using plant extracts for purification of shallow well water in Malawi. *Physics and Chemistry of the Earth, Parts A/B/C*. **34(13-16)**, 799-805.

Lea, M. (2010). Bioremediation of turbid surface water using seed extract from Moringa oleifera Lam.(drumstick) tree. *Current protocols in microbiology*. **1G-2**.

Walter, A., Samuel, W., Peter, A., Joseph, O. (2011). Antibacterial activity of Moringa oleifera and Moringa stenopetala methanol and n-hexane seed extracts on bacteria implicated in water borne diseases. *African Journal of Microbiology Research*. **5(2)**, 153-157.

Kalavathy, M. H., Miranda, L. R. (2010). Moringa oleifera—A solid phase extractant for the removal of copper, nickel and zinc from aqueous solutions. *Chemical Engineering Journal*. **158(2)**, 188-199.

Reddy, D. H. K., Seshaiah, K., Reddy, A. V. R., Lee, S. M. (2012). Optimization of Cd (II), Cu (II) and Ni (II) biosorption by chemically modified Moringa oleifera leaves powder. *Carbohydrate Polymers*. **88(3)**, 1077-1086.

Ho, Y. S., McKay, G. (1999). Pseudo-second order model for sorption processes. *Process biochemistry*. **34(5)**, 451-465.

Avrami, M. (1939). Kinetics of phase change. I General theory. *The Journal of Chemical Physics*. **7(12)**, 1103-1112.

Dalgıç, A.C. (1998). Biogass production from olive residue. A.Ph.D. Thesis. Department of Food Engineering, Gaziantep University.

Plazinski, W., Rudzinski, W., Plazinska, A. (2009). Theoretical models of sorption kinetics including a surface reaction mechanism: a review. *Advances in colloid and interface science*. **152(1-2)**, 2-13.

Langmuir, I. (1918). The adsorption of gases on plane surfaces of glass, mica and platinum. *Journal of the American Chemical society*. **40(9)**, 1361-1403.

Temkin, M. I. (1940). Kinetics of ammonia synthesis on promoted iron catalysts. *Acta physiochim. URSS*. **12**, 327-356.

Dubinin, M. M. (1947). The equation of the characteristic curve of activated charcoal. In *Dokl. Akad. Nauk. SSSR*. (Vol. 55, pp. 327-329).

Freundlich H (1907) Ueber die adsorption in loesungen. Z Phys Chem **57**:385–470.

Çelekli, A., Geyik, F. (2011). Artificial neural networks (ANN) approach for modeling of removal of Lanaset Red G on Chara contraria. *Bioresource technology*. **102(10)**, 5634-5638.

Çelekli, A., İlgün, G., Bozkurt, H. (2012). Sorption equilibrium, kinetic, thermodynamic, and desorption studies of Reactive Red 120 on Chara contraria. *Chemical engineering journal*. **191**, 228-235.

Mahmoodi NM, Hayati B, Arami M, Lan C (2011) Adsorption of textile dyes on pine cone from coloredwastewater: kinetic, equilibriumand thermodynamic studies. Desalination **268**:117–125

Arief, V. O., Trilestari, K., Sunarso, J., Indraswati, N., Ismadji, S. (2008). Recent progress on biosorption of heavy metals from liquids using low cost biosorbents: characterization, biosorption parameters and mechanism studies. *CLEAN–Soil, Air, Water*. **36(12)**, 937-962.

Çelekli, A., Yavuzatmaca, M. (2009). Predictive modeling of biomass production by Spirulina platensis as function of nitrate and NaCl concentrations. *Bioresource technology*. **100(5)**, 1847-1851.

Naveen, N., Saravanan, P., Baskar, G., Renganathan, S. (2011). Equilibrium and kinetic modeling on the removal of Reactive Red 120 using positively charged Hydrilla verticillata. *Journal of the Taiwan Institute of Chemical Engineers*. **42(3)**, 463-469.

Cardoso, N. F., Lima, E. C., Pinto, I. S., Amavisca, C. V., Royer, B., Pinto, R. B., Pereira, S. F. (2011). Application of cupuassu shell as biosorbent for the removal of textile dyes from aqueous solution. *Journal of Environmental Management*. **92(4)**, 1237-1247.

Dawood, S., Sen, T. K. (2012). Removal of anionic dye Congo red from aqueous solution by raw pine and acid-treated pine cone powder as adsorbent: equilibrium, thermodynamic, kinetics, mechanism and process design. *Water research*. **46(6)**, 1933-1946.

Ho, Y. S., McKay, G. (1999). Pseudo-second order model for sorption processes. *Process biochemistry*. **34(5)**, 451-465.

Zwietering, M. H., Jongenburger, I., Rombouts, F. M., Van't Riet, K. (1990). Modeling of the bacterial growth curve. *Applied and environmental microbiology*. **56(6)**, 1875-1881.

Celekli, A., Yavuzatmaca, M., Bozkurt, H. (2009). Kinetic and equilibrium studies on the adsorption of reactive red 120 from aqueous solution on Spirogyra majuscula. *Chemical Engineering Journal*. **152(1)**, 139-145.

Çelekli, A., Bozkurt, H. (2013). Predictive modeling of an azo metal complex dye sorption by pumpkin husk. *Environmental Science and Pollution Research*. **20(10)**, 7355-7366.

Çelekli, A., İlgün, G., Bozkurt, H. (2012). Sorption equilibrium, kinetic, thermodynamic, and desorption studies of Reactive Red 120 on Chara contraria. *Chemical engineering journal*. **191**, 228-235.

Gupta, V. K., Ali, I., Saleh, T. A., Nayak, A., Agarwal, S. (2012). Chemical treatment technologies for waste-water recycling—an overview. *Rsc Advances*. **2(16)**, 6380-6388.

Prola, L. D., Acayanka, E., Lima, E. C., Umpierres, C. S., Vaghetti, J. C., Santos, W. O., Djifon, P. T. (2013). Comparison of Jatropha curcas shells in natural form and treated by non-thermal plasma as biosorbents for removal of Reactive Red 120 textile dye from aqueous solution. *Industrial Crops and Products*. **46**, 328-340.

Reddy, M. S., Sivaramakrishna, L., Reddy, A. V. (2012). The use of an agricultural waste material, Jujuba seeds for the removal of anionic dye (Congo red) from aqueous medium. *Journal of hazardous materials*. **203**, 118-127.

Naveen, N., Saravanan, P., Baskar, G., Renganathan, S. (2011). Equilibrium and kinetic modeling on the removal of Reactive Red 120 using positively charged Hydrilla verticillata. *Journal of the Taiwan Institute of Chemical Engineers*. **42(3)**, 463-469.

Çelekli, A., Yavuzatmaca, M., Bozkurt, H. (2010). Modeling the removal of reactive red 120 on pistachio husk. *CLEAN–Soil, Air, Water*. **38(2)**, 173-180.

Lakshmi, U. R., Srivastava, V. C., Mall, I. D., Lataye, D. H. (2009). Rice husk ash as an effective adsorbent: Evaluation of adsorptive characteristics for Indigo Carmine dye. *Journal of Environmental Management*. **90(2)**, 710-720.

Mane, V. S., Babu, P. V. (2013). Kinetic and equilibrium studies on the removal of Congo red from aqueous solution using Eucalyptus wood (Eucalyptus globulus) saw dust. *Journal of the Taiwan Institute of Chemical Engineers*. **44(1)**, 81-88.

Chen, H., Zhao, J., Wu, J., Dai, G. (2011). Isotherm, thermodynamic, kinetics and adsorption mechanism studies of methyl orange by surfactant modified silkworm exuviae. *Journal of hazardous materials*. **192(1)**, 246-254.

Anirudhan, T. S., Radhakrishnan, P. G. (2008). Thermodynamics and kinetics of adsorption of Cu (II) from aqueous solutions onto a new cation exchanger derived from tamarind fruit shell. *The Journal of Chemical Thermodynamics*. **40(4)**, 702-709.

Adegoke, K. A., Bello, O. S. (2015). Dye sequestration using agricultural wastes as adsorbents. *Water Resources and Industry*. **12**, 8-24.

Yee, A. T. K., Ang, W. F., Teo, S., Liew, S. C., Tan, H. T. W. (2010). The present extent of mangrove forests in Singapore. *Nature in Singapore*. **3(3)**, 139-145.

Sumathi, P., Parvathi, A. (2010). Antimicrobial activity of some traditional medicinal plants. *Journal of Medicinal plants research*. **4(4)**, 316-321.

Tan, B. K., Adya, R., Randeva, H. S. (2010). Omentin: a novel link between inflammation, diabesity, and cardiovascular disease. *Trends in cardiovascular medicine*. **20(5)**, 143-148.

Reddy, M. V., Subba Rao, G. V., Chowdari, B. V. R. (2013). Metal oxides and oxysalts as anode materials for Li ion batteries. *Chemical reviews*. **113(7)**, 5364-5457.

Çelekli, A., Çelekli, F., Çiçek, E., Bozkurt, H. (2014). Predictive modeling of sorption and desorption of a reactive azo dye by pumpkin husk. *Environmental Science and Pollution Research*. **21(7)**, 5086-5097.